

1 **Reactivity of chlorine radical with submicron palmitic acid** 2 **particles: kinetic measurements and product identification**

3 Maxence Mendez¹, Raluca Ciuraru^{1,*}, Sylvie Gosselin¹, Sébastien Batut¹, Nicolas Visez¹,
4 Denis Petitprez¹

5 [1]{Laboratoire Physicochimie des Processus de Combustion et de l'Atmosphère (PC2A)
6 UMR CNRS 8522 Université Lille 1, F-59655, Villeneuve d'Ascq, France}

7 [*]{now at: IRCELYON, Institut de Recherches sur la Catalyse et l'Environnement de Lyon,
8 CNRS UMR 5256, Université Lyon 1, F-69626 Villeurbanne Cedex, France}

9 Correspondence to: D. Petitprez (denis.petitprez@univ-lille1.fr)

10

11 Abstract

12 The heterogeneous reaction of Cl[•] radicals with sub-micron palmitic acid (PA) particles was
13 studied in an aerosol flow tube in the presence or in the absence of O₂. Fine particles were
14 generated by homogeneous condensation of PA vapours and introduced in the reactor where
15 chlorine atoms were produced by photolysis of Cl₂ using UV lamps surrounding the reactor.
16 The effective reactive uptake coefficient (γ) has been determined from the rate loss of PA
17 measured by GC/MS analysis of reacted particles as a function of the chlorine exposure. In
18 the absence of O₂, $\gamma = 14 \pm 5$ indicates efficient secondary chemistry involving Cl₂. GC/MS
19 analysis have shown the formation of monochlorinated and polychlorinated compounds in the
20 oxidized particles. Although the PA particles are solid, the complete mass can be consumed.
21 In the presence of oxygen, the reaction is still dominated by secondary chemistry but the
22 propagation chain length is smaller than in the absence of O₂ which leads to an uptake
23 coefficient $\gamma = 3 \pm 1$. In the particulate phase, oxocarboxylic acids and dicarboxylic acids
24 were identified by GC/MS. Formation of alcohols and monocarboxylic acids is also
25 suspected. A reaction pathway for the main products and more functionalized species is
26 proposed. All these results show that solid organic particles could be efficiently oxidized by
27 gas-phase radicals not only on their surface, but also in bulk by mechanisms which are still
28 unclear. They help to understand the aging of primary tropospheric aerosol containing fatty
29 acids.

1 **1 Introduction**

2 The concentration of organic matter in marine environments exhibits a seasonal behaviour,
3 which dominates the chemical composition of fine particulate matter during periods of high
4 biological activity (Yoon *et al.*, 2007;O'Dowd *et al.*, 2004;Cavalli *et al.*, 2004;Sciare *et al.*,
5 2008). Cells of living organisms in the oceans decompose after their death and the
6 hydrophobic cellular constituents accumulate on the water surface forming a sea-surface
7 micro-layer of 1 to 1,000 μm thickness (Hardy, 1982). When sea-salt aerosols (SSA) are
8 generated by the mechanical ejection of droplets from waves and winds, these organic
9 compounds are also ejected, thus becoming a component of the newly formed particles
10 (Barger and Garrett, 1976;Gogou *et al.*, 1998;Marty *et al.*, 1979). Recent laboratory and field
11 measurements have shown that the organic mass fraction of SSA increases from 0.1 to near 1
12 when the ambient aerosol aerodynamic diameter decreases from 1 to 0.1 μm (Keene *et al.*,
13 2007;Facchini *et al.*, 2008). The exact mechanism for such large organic mass fraction of
14 submicron SSA is not well understood.

15 Chemical analysis of organic compounds sampled in SSA have allowed to identify fatty acid
16 (C12-C18) compounds (Marty *et al.*, 1979), contributing to up to 10% in mass of the total
17 organic content of the particles (Mochida *et al.*, 2002).

18 Molecular characterizations of sea-salt aerosols collected in marine air masses have shown
19 that fatty acids (FA) consist of relatively short carbon chains (Tervahattu *et al.*,
20 2002b;Tervahattu *et al.*, 2002a;Mochida *et al.*, 2002;Oros and Simoneit, 2001). Due to the
21 hydrophobic properties of surfactants, the fatty acids are thought to form an organic coating
22 around the inorganic core of the particles (Ellison *et al.*, 1999;Rudich, 2003). When
23 considering a monolayer coating, the surface coverage by FA is estimated to be on the order
24 of 0.3 to 14% (Tervahattu *et al.*, 2005;Mochida *et al.*, 2002).

25 Fatty acids are also ubiquitous in airborne particles sampled in urban atmospheres (Oliveira *et*
26 *al.*, 2007). They were found to contribute to up to 50% of identified organic compounds from
27 emission sources such as biomass burning (Nolte *et al.*, 2001;Schauer *et al.*, 2001;Fine *et al.*,
28 2001), cooking (Schauer *et al.*, 2002;He *et al.*, 2004), and automobiles (He *et al.*, 2006).
29 Among the fatty acids, palmitic acid ($\text{C}_{16}\text{H}_{32}\text{O}_2$) is the most abundant
30 one (Mochida *et al.*, 2002).

1 Recent literature reviews have presented the physical and chemical processes which occur at
2 the interface of airborne organic particles (Donaldson and Vaida, 2006;Rudich, 2003;George
3 and Abbatt, 2010). Many heterogeneous reactions of atmospheric particles involve the main
4 oxidant of the atmosphere (*i.e.* the hydroxyl radical OH[·]) which chemically alters their
5 surfaces thus aging them. The intensity of this aging depends on various parameters such as
6 meteorological conditions, size of the particle, and the chemical composition of the particle
7 surface and bulk. Consequently, variability of these parameters leads to the observed spatial
8 and temporal variability of the physical and chemical properties of atmospheric aerosols.
9 These heterogeneous processes affect the optical, hygroscopic and reactive properties of
10 airborne particles thereby making uncertain the prediction of their global and regional
11 atmospheric impact. Although the OH[·] radical is the primary daytime oxidant, halogen atoms
12 (Cl, Br and I) may also significantly participate in oxidation processes, especially in the
13 marine boundary layer (MBL). Halogen species are emitted from anthropogenic sources, but
14 important sources are also represented by the halogen-release from sea-salt aerosols and
15 associated heterogeneous reactions. Cl[·] atoms are mainly generated from the photolysis of
16 active chlorine species and their concentrations can be up to 10⁶ atom.cm⁻³ (Spicer *et al.*,
17 1998;Pechtl and von Glasow, 2007).

18 Recent atmospheric measurements (Osthoff *et al.*, 2008) have shown that nitryl chloride
19 (ClNO₂) is produced by heterogeneous reactions on sea-salt particles and accumulates during
20 the night. At dawn, the photolysis of nitryl chloride produces a peak of Cl[·] with an estimated
21 rate of formation of 1×10⁶ atom cm⁻³ s⁻¹.

22 This Cl[·] atom source seems modest relative to other oxidants. However, it has been reported
23 that Cl[·] reacts faster than OH[·] radicals with hydrocarbon compounds (Spicer *et al.*, 1998) and
24 may represent the major oxidant of the troposphere in coastal and industrialized areas,
25 especially at dawn, when concentrations of OH[·] radicals are low. While sources of reactive
26 halogen species and halogen chemistry in the troposphere are relatively well studied, detailed
27 chemical processes are still unknown (George and Abbatt, 2010).

28 Given the high reactivity of Cl[·] atoms with organic compounds and the ubiquity of Cl[·] and
29 fatty acids in the troposphere, especially in the MBL, it is obvious that this heterogeneous
30 reactivity must be considered. However, only a few experimental studies between gas-phase
31 radicals (Cl[·] or OH[·]) with condensed-phase organic compounds, including model organic
32 surfaces, are reported.

1 Uptake coefficients of OH[·] on pure palmitic acid (PA) particles between 0.8 and 1 have been
2 reported by McNeill *et al.* (McNeill *et al.*, 2008). The authors also measured uptake
3 coefficients for thin PA film coatings on solid and liquid NaCl particles, obtaining lower
4 values than for pure PA experiments (solid, $\gamma^{\text{OH}} \approx 0.3$ and liquid, $\gamma^{\text{OH}} \approx 0.05$). Experiments
5 with chlorine atoms, generated from Cl₂ photolysis, have also been considered as a model for
6 radical-initiated oxidation chemistry which avoids the presence of reactive precursors or side-
7 products during generation of OH[·]. The reactive uptake of Cl[·] atoms on self-assembled
8 organic monolayers was studied by Moise and Rudich (Moise and Rudich, 2001) using a flow
9 reactor coupled to a chemical ionization mass spectrometer. The uptake coefficient, measured
10 by recording the rate of loss of Cl[·] radicals, was estimated to be in the range ($0.1 < \gamma < 1$), close
11 to the diffusion-limited loss rate.

12 Reactions of Cl[·] radicals in the presence of O₂ have been studied using an aerosol flow tube
13 to stand as a model of the radical-initiated oxidation of liquid phase organic aerosols. In the
14 case of reactions of Cl[·] radicals with dioctyl sebacate (DOS) particles (Hearn *et al.*, 2007), in
15 the presence of O₂, uptake coefficient has been determined by monitoring the rate of loss of
16 DOS species. The uptake coefficient exhibits a value greater than unity ($\gamma_{\text{DOS-OH}} = 1.7 \pm 0.3$)
17 indicating a radical chain chemistry. Products were mainly identified in the particles, showing
18 an inefficient volatilization process.

19 More recently, heterogeneous reactions between Cl[·] atoms and submicron squalane particles
20 have been investigated in a photochemical aerosol flow tube (Liu *et al.*, 2011). Secondary
21 chain chemistry occurring in the liquid phase has also been demonstrated during this study.
22 The measured uptake coefficient decreases from a value of ~ 3 for experiments performed
23 without O₂ to a value of 0.65 for experiments in the presence of O₂. Product formation in
24 condensed phase is controlled by competitive reaction rates of O₂ and Cl₂ with alkyl radicals.

25 All of these studies of heterogeneous reaction between radical species and organic surfaces or
26 particles as a model for the oxidation of organic aerosols clearly emphasize the role of OH[·] or
27 Cl[·] in initiating oxidation processes *via* an H-abstraction pathway. This is followed by a chain
28 reaction which can accelerate the overall rate of particle transformation. Concerning
29 experiments with Cl[·] radicals, it was shown that more than 60% of the initial condensed
30 matter can be consumed by the reactions. Several hypotheses have been put forth to explain
31 these surprising observations: (1) a quite rapid surface renewal process, (2) an efficient
32 secondary chain chemistry in the bulk. These processes might readily occur in the case of

1 liquid droplets (DOS or squalane) but are limited by the diffusion of the species in the liquid
2 phase for both reactants and products. In the case of solid particles, surface renewal can be
3 induced by volatilization. Trapping of species within the particle or phase change of the
4 surface layer cannot be excluded.

5 Chemical mechanisms adapted from the homogeneous phase have been proposed to interpret
6 the formation of products mainly in the particulate phase but reaction pathways still remain
7 unclear due to the specificity of the condensed phase (microscopic arrangement of the
8 molecules, diffusion process in liquid/solid phase, for example).

9 We present here the experimental results of heterogeneous reactivity between Cl^\cdot and PA
10 within an Aerosol Flow Tube (AFT) where fine particles generated by homogeneous
11 condensation of PA vapours are introduced with Cl_2 as a radical precursor. Cl^\cdot atoms are
12 generated by photolysis of the molecular chlorine using UV lamps surrounding the reactor.
13 Experiments have been conducted with and without O_2 . For both cases, uptake coefficients
14 have been determined by monitoring the decay of PA by GC/MS analyses of collected
15 particles on filters at the exit of the reactor. Identification of the reaction products in the
16 condensed phase have been performed by GC/MS analyses and has led to the proposal of a
17 detailed chemical mechanism for oxidation of carboxylic acids in particulate matter.

18 **2 Experimental section**

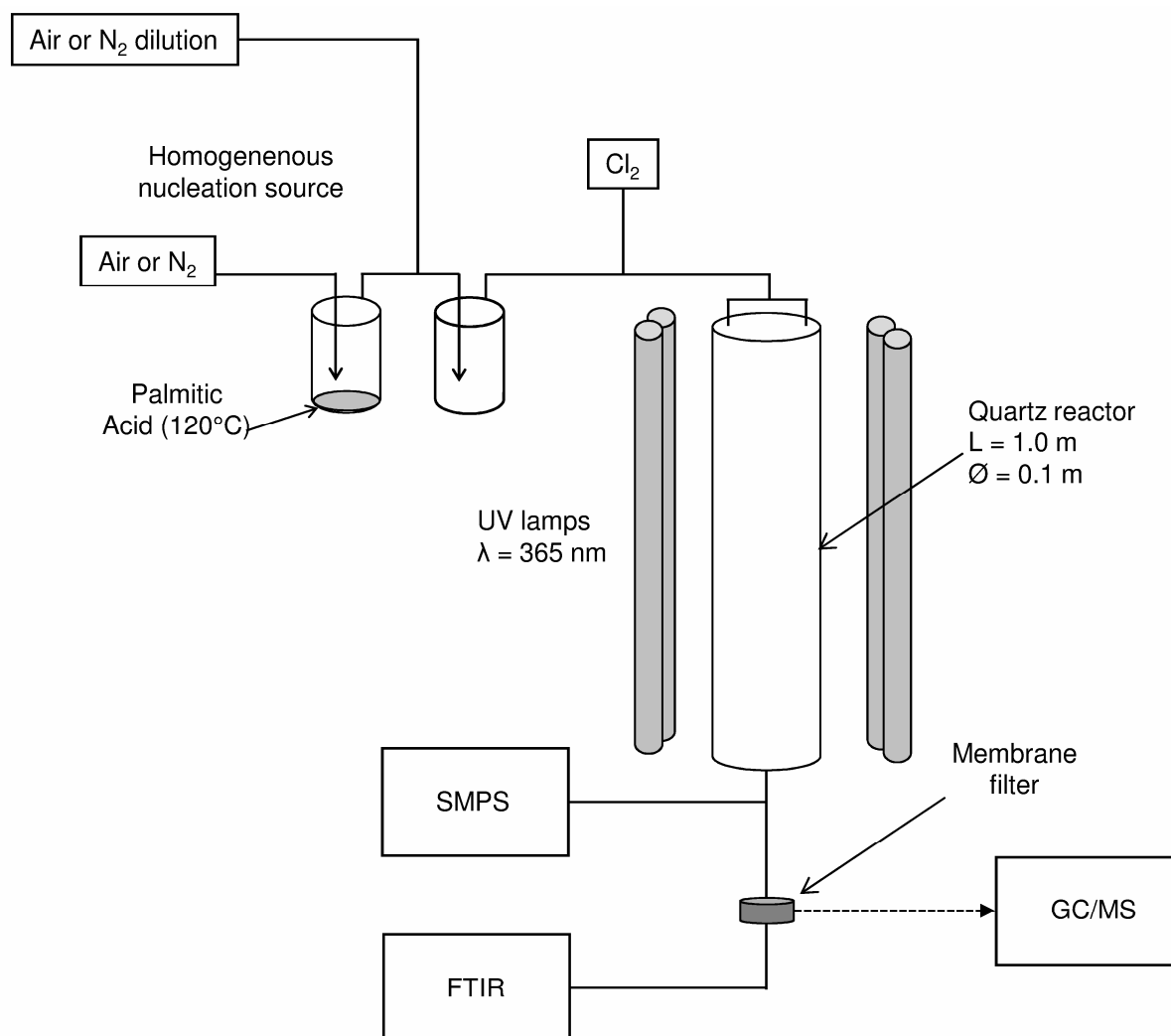
19 ***2.1 Aerosol flow tube***

20 An atmospheric pressure aerosol flow tube (AFT) is used to investigate the heterogeneous
21 reactivity of PA particles with chlorine atoms (Fig. 1). The AFT is a 1 m long and 10 cm
22 inner diameter quartz tube surrounded by 8 UV lamps (UVP, 365 BLB, $\lambda_{\text{mean}} = 365$ nm). The
23 particles and the gas-phase oxidant precursor are introduced into the upper flange of the
24 reactor through two $\frac{1}{4}$ " stainless steel connectors. The total flow, monitored by mass flow
25 meters, is fixed at 4.0 L min^{-1} which corresponds to a mean residence path time of 180 s in the
26 AFT.

27 ***2.2 Reactant generation***

28 Palmitic acid ($\geq 98\%$) is purchased from Roth. Chemical purchased from Aldrich is:
29 dichloromethane (99.8%). Chemicals from Fluka are: tetradecane ($\geq 98\%$), hexadecane (\geq

1 98%). N,O-Bis (trimethylsilyl) trifluoroacetamide, $C_8H_{18}F_3NOSi_2$ - Trimethylchlorosilane
2 (BSTFA-TMCS) (99%-1%) solution is purchased from Supelco. Gases are purchased from
3 Praxair: Synthetic air 3.0, Nitrogen 4.6. Chlorine (1% of Cl_2 in Helium) is purchased from Air
4 Liquide (99.6%).



5
6 Figure 1. Experimental setup, SMPS (Scanning Mobility Particle Sizer), FTIR (Fourier
7 Transform InfraRed spectrometer), GC/MS (Gas Chromatography, Mass Spectrometer)

8 **2.3 Particle generation**

9 Palmitic acid particles are generated by homogeneous nucleation in a stream of 1 L min^{-1} N_2
10 or N_2/O_2 flowing through a glass vessel containing 5 grams of PA. A heating wire wraps the
11 glass vessel and the PA temperature is kept constant ($\pm 1^\circ C$) using a temperature controller.
12 The flow is diluted with 1 L min^{-1} of N_2 or N_2/O_2 and sent to a condensation tube of 1.5 L
13 volume at room temperature. The size distribution of the particles is continuously recorded by

1 a SMPS (model TSI 3080L) every 2 minutes. Palmitic acid particle density was assumed to be
 2 the solid phase density ($d=0.852 \text{ g cm}^{-3}$). Depending on the heating temperature and flows,
 3 mass concentrations between 500 and 1,000 $\mu\text{g m}^{-3}$ of PA particles are generated. For a
 4 temperature of around 120°C, the setup produces a log-normal particle size distribution with a
 5 mean surface-weighted diameter of $\sim 500 \text{ nm}$ and a geometric standard deviation of ~ 1.5 .
 6 Measuring the aerosol concentration before and after the AFT has revealed that the mean
 7 diameter is not modified and that at maximum a mass loss of 10% occurred while passing
 8 through the AFT.

9 **2.4 Atomic chlorine production**

10 The chlorine radicals are generated along the length of the AFT by powering all or some of
 11 the 8 UV lamps. The Cl concentration can also be adjusted by controlling the Cl_2 initial
 12 concentration in the AFT.

13 The chlorine radical concentration is measured by performing reference kinetic experiments
 14 with acetone. Molecular chlorine (3 to 20 ppm) and acetone (50 ppm) are introduced in the
 15 reactor and the reaction between acetone and Cl takes place with a second order rate constant
 16 (k_{ref}) of $2.09 \times 10^{-12} \text{ cm}^3 \text{ molecule}^{-1} \text{ s}^{-1}$ (Liu *et al.*, 2011; George *et al.*, 2007). The loss of
 17 acetone is monitored by Fourier transform infrared (FTIR) spectroscopy by integration of the
 18 absorbance of the C-C stretching band at $1,217 \text{ cm}^{-1}$ (Perelygin and Klimchuk, 1974) between
 19 $1,160$ and $1,260 \text{ cm}^{-1}$. The loss rate of acetone can be expressed as:

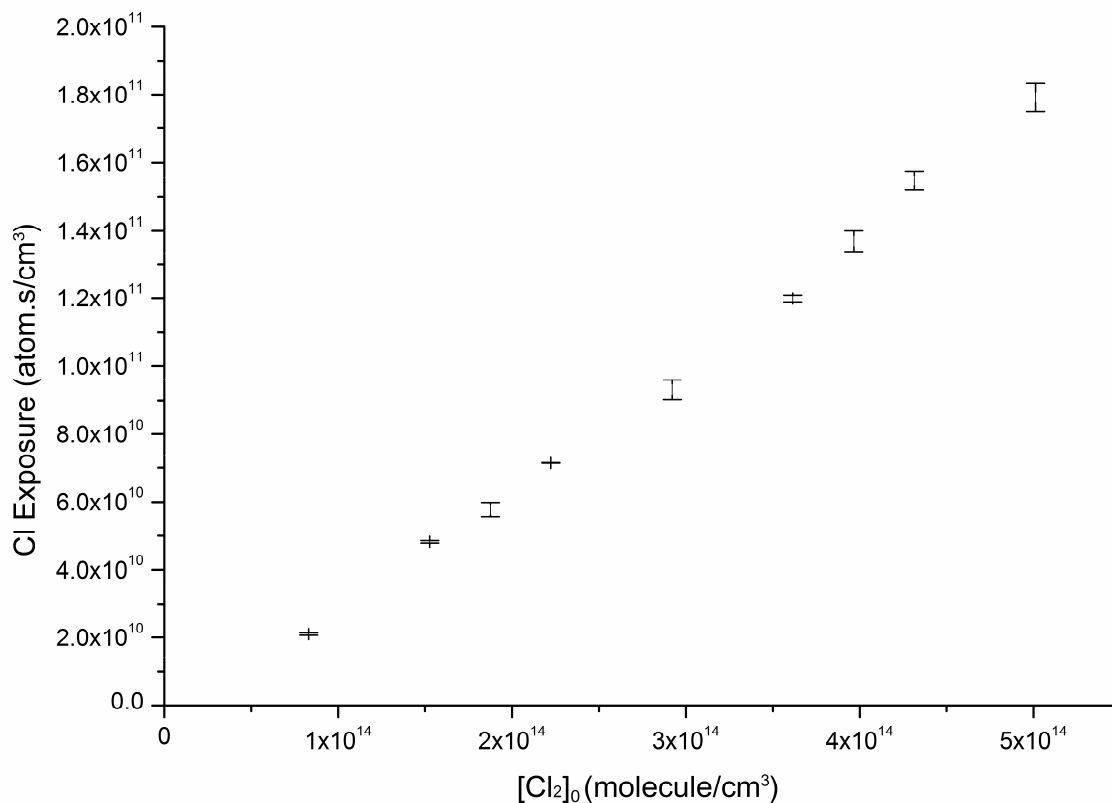
$$20 \quad v = \frac{d[Acet]}{dt} = -k_{ref} [Acet][Cl] \quad (1)$$

21 Integration of Eq (2) leads to determination of the chlorine exposure ($\langle Cl \rangle_{t,t}$ in $\text{atom cm}^{-3} \text{ s}$)
 22 which is the product of the reaction time t with the time averaged chlorine radical
 23 concentration along the reactor $\langle Cl \rangle_t$, where $[Acet]_0$ and $[Acet]_t$ are the initial and final
 24 concentrations of acetone measured by FTIR spectroscopy respectively.

$$25 \quad \frac{\ln \frac{[Acet]_t}{[Acet]_0}}{-k_{ref}} = \int_0^t [Cl] dt = \langle Cl \rangle_t \cdot t \quad (2)$$

26 As shown in Fig. 2, the chlorine exposure, $\langle Cl \rangle_{t,t}$, is linearly proportional to $[\text{Cl}_2]$ with a
 27 maximum time averaged chlorine concentration of $2.25 \times 10^9 \text{ atom cm}^{-3}$. The ratio $[\text{Cl}_2]/[\text{Cl}]$

1 expresses the photodissociation efficiency and is greater than 3,000 and means that on
2 average one Cl₂ out of 6,000 is dissociated by photolysis and produces 2 Cl[·] radicals.



3
4 Figure 2. Chlorine exposure as function of the initial Cl₂ concentration in the reactor; Q_{tot} =
5 4.0 L min⁻¹ and 8 UV lamps powered. Errors bars express the minimum and maximum values
6 of 4 experiments.

7 **2.5 Analytical procedure**

8 **2.5.1 Particle sampling and GC/MS analysis.**

9 At the reactor outlet, the particles are sampled on a PTFE (PolyTetraFluoroEthylene) filter
10 (Millipore FALP, 1.0 μm, diameter 47 mm) for 10 minutes in order to collect about 20 μg of
11 PA. The filter is then placed in a 1.5 mL vial and 10 μL of a solution containing two internal
12 standards (tetradecane and hexadecane) and 25 μL of a commercial mixture 99% BSTFA /
13 1% TMCS are deposited directly on the membrane. Quantitative analysis of carboxylic acids
14 by gas chromatography requires derivatization of the -COOH function. Silylation by BSTFA
15 (N, O-Bis (trimethylsilyl) trifluoroacetamide, C₈H₁₈F₃NOSi₂) has been previously used for the
16 determination of mono- and dicarboxylic acids in samples of atmospheric particles collected

1 on filters (Docherty and Ziemann, 2001; Wang *et al.*, 2009; Zuo *et al.*, 2007; Yu *et al.*, 1998).
2 Trimethylchlorosilane (TMCS) acts as a catalyst by increasing the silyl donor strength of the
3 BSTFA. After finally adding a volume of 1 mL of dichloromethane, the filter is subjected to
4 10 minutes of sonication. For the product identification, only a volume of 200 μL of
5 dichloromethane is added before the sonication. NIST mass spectra database (V2.2) is used
6 for the identification. After the extraction and silylation steps, 1 μL of the solution is injected
7 in a Gas Chromatograph Mass Spectrometer (Perkin-Elmer GC Clarus 680). The
8 chromatographic conditions are as follows: inlet 250°C, split mode 5 mL min⁻¹, constant
9 column flow 1 mL min⁻¹, oven temperature: 50°C for 0.5 min, ramp +20°C min⁻¹ to the final
10 temperature 310°C. Separation is provided by an Elite-5MS 30 meter long column (diameter
11 250 μm and film thickness 0.5 μm). Identification and quantification is performed on a Clarus
12 600C mass spectrometer in 70 eV electron impact mode with a source temperature of 180°C.

13 The quantification of palmitic acid is done by injecting standard solution of known
14 concentration. The ion fragment corresponding to the silyl group Si(CH₃)₃ (m/z=73) is chosen
15 for the quantification of silylated palmitic acid. All samples are injected in triplicates in
16 Selected Ion Monitoring (SIM) mode for the quantification and once in scan mode for
17 identification. The mass of PA particles collected on the filter for 10 minutes was quantified
18 by GC/MS and compared to the mass concentration measured by the SMPS analysis during
19 the same period. It appears that the mass derived from GC/MS represents 80 % \pm 10 % of the
20 mass as determined by the SMPS. These measurements have been performed without UV
21 radiations so without Cl^o radicals in the AFT. Among the causes that can explain these
22 differences, we can surely mention: - efficiency of the extraction of palmitic acid before
23 GC/MS analyses, - errors from the SMPS which is a non-absolute technique for mass
24 determination due to many assumptions introduce in the SMPS data process (shape and
25 density of the particles) and other error sources as the calibration of the particles counter.

26 2.5.2 FTIR analysis

27 Gas phase analysis were performed by Fourier transform infrared spectroscopy mainly for the
28 chlorine exposure determination. The FTIR spectra are recorded with an Avatar–Thermo
29 Scientific spectrometer equipped with a 10 m length multipath cell. Each spectrum is obtained
30 while averaging 100 scans in the 400 – 4,000 cm⁻¹ spectral range with a spectral resolution of
31 1 cm⁻¹. Background spectra are taken before and after reactivity experiments to make sure that
32 measured products are not stuck on the mirrors of the cell.

1 **3 Results and discussion**

2 **3.1 Chlorine reactivity in N₂**

3 3.1.1 Kinetic measurements

4 First, we studied the heterogeneous oxidation of palmitic acid particles by Cl radicals in an
5 O₂-free environment. The classical parameter determined in heterogeneous kinetic
6 measurements is the reactive uptake coefficient γ_{Cl} which is defined as the fraction of Cl
7 collisions with the particle leading to the loss of Cl in the gas-phase. Since the loss of Cl is not
8 measured in this experiment, the reaction is monitored through the reactive loss of palmitic
9 acid in the particle phase γ_{PA} . The PA loss rate can be expressed as follows:

$$10 \quad \frac{d[PA]}{dt} = -k_{PA} [Cl][PA] \quad (3)$$

11 where k_{PA} is the second order rate constant of PA with Cl (cm³ molecule⁻¹ s⁻¹). [PA] and [Cl]
12 are the time dependent concentrations of the reactants (molecule cm⁻³). The palmitic loss ϕ_{loss}
13 (molecule s⁻¹ cm⁻²) is defined by:

$$14 \quad \phi_{loss} = \frac{V}{S_p} k_{PA} [Cl][PA] \quad (4)$$

15 where S_p is the particle surface density (cm² cm⁻³) and V the volume of the particle. The flux
16 of collisions ϕ_{coll} (molecule s⁻¹ cm⁻²) occurring on the particle surface per second is expressed
17 in the equation 5:

$$18 \quad \phi_{coll} = \frac{[Cl] \cdot \omega_{Cl}}{4} \quad (5)$$

19 where ω_{Cl} is the mean speed of gas-phase Cl (cm s⁻¹). The integration of equation 3 leads to:

$$20 \quad k_{PA} = \frac{\ln \frac{[PA]_0}{[PA]_t}}{\langle Cl \rangle_t \cdot t} \quad (6)$$

21 [PA]₀ and [PA]_t are the initial and final concentrations of particle-phase PA, respectively, and
22 measured by GC/MS (molecule cm⁻³). $\langle Cl \rangle_{t,t}$ (atom cm⁻³ s) is the exposure obtained by the
23 reference kinetics measurements and k_{PA} is experimentally determined from the decay of

1 palmitic acid as a function of the exposure. Moreover, $[PA]_0$ can be replaced in the uptake
 2 coefficient expression by:

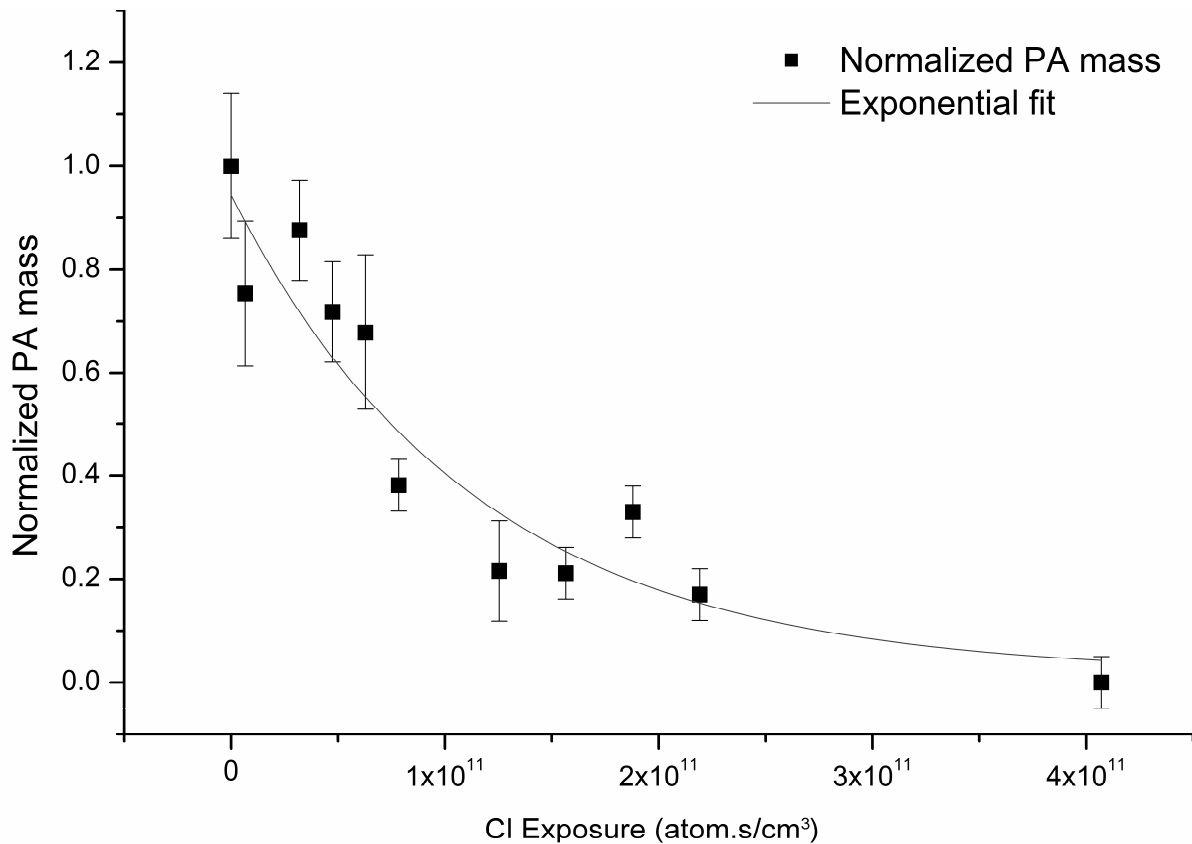
$$3 \quad [PA]_0 = \frac{V_P \cdot \rho_{PA} \cdot N_A}{M_{PA}} \quad (7)$$

4 where V_P is the particle volume density ($\text{cm}^3 \text{cm}^{-3}$), M_{PA} is the molar mass of palmitic acid
 5 ($M_{PA} = 256 \text{ g.mol}^{-1}$), ρ_{PA} is the palmitic acid density ($\rho_{PA} = 0.852 \text{ g.cm}^{-3}$) and N_A is the
 6 Avogadro's number. Finally, the uptake coefficient γ_{PA} can be expressed as:

$$7 \quad \gamma_{PA} = \frac{\varphi_{loss}}{\varphi_{coll}} = \frac{4 \cdot k_{PA} \cdot D_{mean} \cdot \rho_{PA} \cdot N_A}{\omega_{Cl} \cdot 6 \cdot M_{PA}} \quad (8)$$

8 D_{mean} is the mean surface-weighted diameter of the particle distribution and is calculated by
 9 $V_P/S_P = D_{mean}/6$ (Smith *et al.*, 2009). The mean particle diameter is determined by SMPS
 10 measurements and is assumed to be constant and equal to the initial mean particle diameter.

11 The normalized decay of ($[PA]_t/[PA]_0$) as a function of Cl exposure is shown in Fig. 3. The
 12 decay constant k_{PA} is obtained from an exponential fit to the experimental measurements for
 13 exposure values ranging from 0 to $4 \times 10^{11} \text{ molecule cm}^{-3} \text{ s}$.



14

1 Figure 3. Normalized mass of PA remaining in particles collected on filter during 10 minutes
2 as a function of the chlorine exposure (squares). Each data point is a mean value obtained
3 from three GC/MS analyses of two particles samples; errors bars represent minimum and
4 maximum values. The data have been fitted by an exponential function (solid line).

5 Using the rate constant k_{PA} ($k_{PA} = 1 \cdot 10^{-11} \text{ molecule}^{-1} \text{ cm}^3 \text{ s}^{-1}$) obtained from the slope of the
6 exponential fit of kinetic data in Fig. 3, the initial uptake coefficient γ_{PA} has been determined
7 to be equal to 14 ± 5 in an oxygen-free environment. Using the model developed by Fuchs
8 and Sutugin (Fuchs and Sutugin, 1970), the calculation of the gas-phase diffusion limitation
9 leads to a correction of 10% for γ which is smaller than the total error from the experiment
10 setup. The high value of γ means that: (1) the heterogeneous reaction of PA with Cl radical is
11 very efficient; (2) the secondary chemistry is leading the overall reaction. These results are
12 similar to those of Liu *et al.* (Liu *et al.*, 2011) who reported $\gamma = 3$ for the uptake coefficient of
13 chlorine on squalane particles. However, Liu *et al.* determined the loss of squalane as a
14 function of the total chlorine radical concentration while, in this study, the loss of palmitic
15 acid is measured as a function of the chlorine radical concentration produced only from the
16 photolysis of Cl_2 . As a result, the uptake coefficients cannot be strictly compared but both
17 show the importance of secondary chemistry.

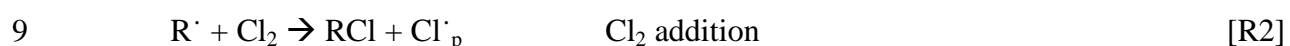
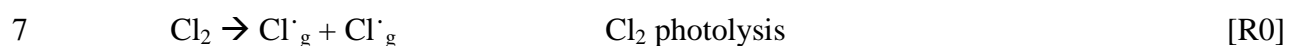
18 By definition, the initial uptake coefficient, when derived from the measurement of the rate
19 loss of the gas phase oxidant Cl_g , γ_{Cl} , cannot be greater than 1. Here the uptake coefficient,
20 determined from the rate loss of the condensed phase (γ_{PA}) is significantly greater than one
21 ($\gamma_{PA} = 14 \pm 5$), indicating an efficient secondary heterogeneous chemistry leading the whole
22 reaction. The chain propagation length is the ratio between the number of palmitic acid
23 molecules lost and Cl_g atoms that react and corresponds to the ratio γ_{PA}/γ_{Cl} . The chain
24 propagation length is at least equal to 14.

25 Although, the palmitic acid particles are solid, the complete palmitic acid mass can be almost
26 completely consumed. This behavior has already been observed for heterogeneous chemistry
27 involving liquid compounds where diffusion in the bulk can be suggested as an explanation
28 for fast refreshing of the surface. In the case of solid particles, this surprising observation is
29 somehow more difficult to discuss. Two hypotheses can be put forward: (1) an efficient
30 volatilization of the products formed at the surface of the particle or, (2) a phase change of the

1 first layers facilitating diffusion or trapping of species within the particle (McNeill *et al.*,
2 2008; Marcolli *et al.*, 2004; Garton *et al.*, 2000).

3 3.1.2 Reaction mechanism

4 The high value of the uptake coefficient confirms that the PA consumption is enhanced by
5 secondary chemistry. Liu *et al.* proposed a catalytic mechanism which can be adapted to our
6 oxidation process.

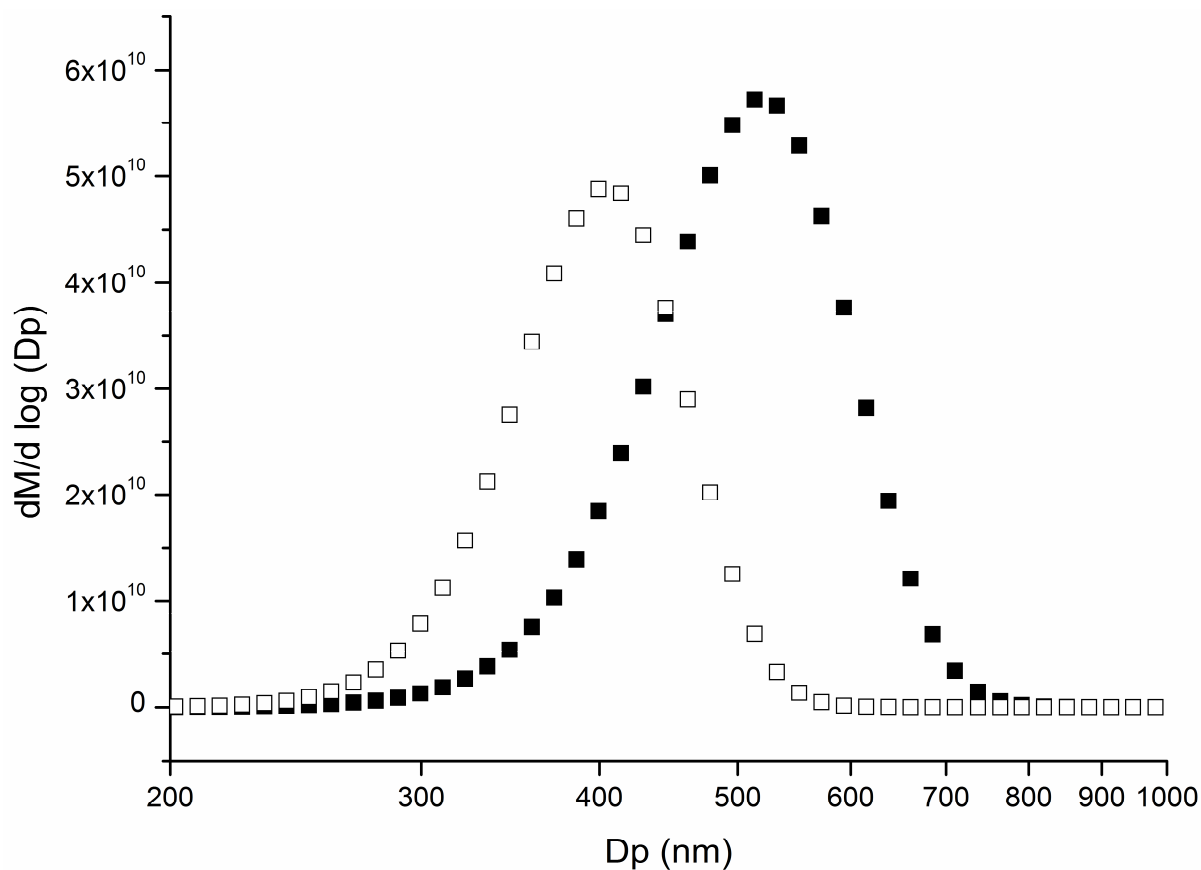


14 Cl'_{g} is defined as a gas phase Cl' produced from Cl_2 photolysis. The initiation reaction [R1] is
15 the heterogeneous reaction between Cl'_{g} and particle-phase PA at the surface of the particle
16 producing an alkyl radical R' . A chlorine molecule can be added on the R' leading to
17 formation of a chlorinated product and atomic chlorine Cl'_{p} . This chlorine atom is released
18 from the surface of the particle and can easily react with another hydrocarbon. R4, R5 and R6
19 are reactions terminating the radical chain propagation. R6 could occur heterogeneously via
20 the collision between Cl'_{g} and Cl'_{p} but also can take place in the condensed phase and involve
21 two Cl'_{p} . Such heterogeneous mechanism has already been observed in previous studies
22 performed either on NaCl particles (Ciuraru *et al.*, 2011) or on ammonium sulphate particles
23 (Ciuraru *et al.*, 2012). The reaction rate of [R1] is defined by the uptake coefficient of
24 chlorine on the particle surface γ_{Cl} . R2 is a source of Cl' allowing the chlorine radical
25 concentration to be renewed; moreover the $[\text{Cl}_2]$ concentration is in excess of $[\text{Cl}']$ ($[\text{Cl}_2]/$
26 $[\text{Cl}'] > 3,000$).

27 3.1.3 Change in the particle size distribution

28 The SMPS data indicate that the initial log-normal particle distribution mean diameter shifts
29 from 520 to 405 nm after a Cl-exposure of 1.25×10^{11} molecule cm^{-3} s (see Fig. 4). For this

1 specific exposure, the aerosol mass measured by SMPS decreases by 40% whereas the
2 GC/MS analysis shows that 80% of the particle-phase PA is lost. Chlorinated products have a
3 higher molar mass than PA and it is assumed that they remain in the condensed phase, thus
4 changing the density of oxidized particles compared to initial pure PA particles. The oxidized
5 particle diameter cannot therefore be rigorously determined because the particle diameter is
6 obtained from electrical mobility of the particle which depends on their density. Assuming
7 that the change of the mean diameter is only due to the density variation would indicate that
8 the particle density would have increased from 0.852 to 1.850. This value seems too high for
9 an organic compound and suggests that the mean diameter change is also due to volatilization
10 of products. Consequently, the initial mean surface-weighted particle diameter is considered
11 in this following kinetic study.



12
13 Figure 4. Mass-weighted particle distribution (normalized $\mu\text{g m}^{-3}$) of PA particles before
14 (filled squares) and after (open squares) a chlorine exposure of $1.25 \times 10^{11} \text{ atom cm}^{-3} \text{ s}$. Each
15 distribution is an average of eight measurements.

1 3.1.4 Particulate-phase product identification

2 Evidence of presence of monochlorinated palmitic acid is found in the mass spectra.
3 Fragments with $m/z=362$ and 364 are detected and correspond to the parent peaks of the
4 silylated monochlorinated palmitic acid ($C_{15}H_{30}Cl-COO-Si-(CH_3)_3$) with characteristic pattern
5 for the $m/z=35$ and 37 isotopic relative abundances of chlorine. In those mass spectra, the
6 presence of the peak $m/z=117$ (corresponding to $-COO-Si-(CH_3)_3$) shows that the carboxylic
7 acid function has not been modified and the chlorine atom has not been added on the oxygen
8 atom. Because the hydrogen abstraction by chlorine can occur at 17 different sites, several
9 monochlorinated products are detected instead of one single product.

10 Dichlorinated palmitic acid molecules are also detected in the sampled particles. The
11 formation of different constitutional isomers induces much smaller peaks than the
12 monochlorinated ones. The mass spectra of those species shows the $m/z=396$, 398 and 400
13 amu, indicating the presence of the parent peak of $C_{15}H_{29}Cl_2-COO-Si-(CH_3)_3$ with the natural
14 abundance of chlorine atoms. The mass spectra of those species indicates the presence of the
15 silylated monochlorinated palmitic acid fragment ($m/z=362$ and 364) and also the silylated
16 carboxylic acid function. Polychlorinated palmitic acid molecules such as trichlorinated
17 palmitic acid molecules and more are highly suspected but the signal/noise ratios are too low
18 to get unambiguous identifications.

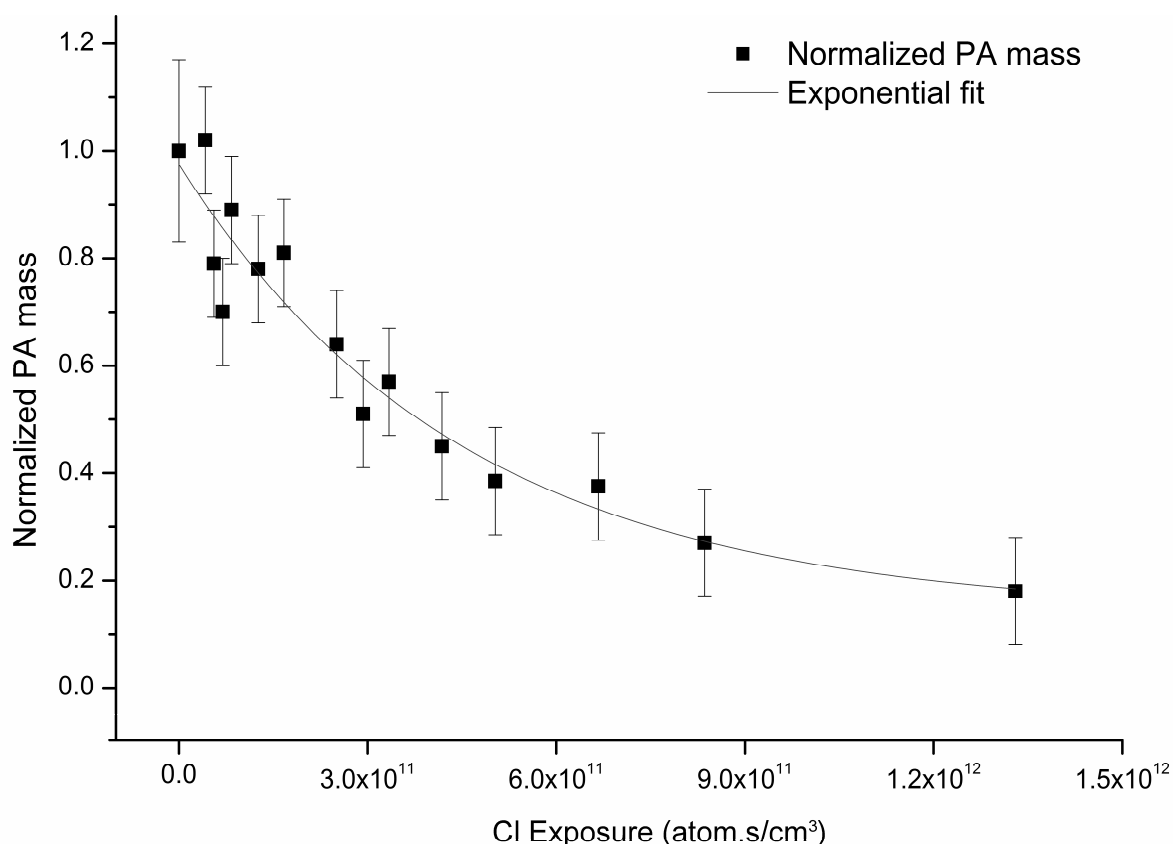
19 **3.2 Chlorine reactivity in the presence of O_2**

20 3.2.1 Kinetic measurements

21 The effect of oxygen on the heterogeneous reactivity between Cl^{\bullet} atoms and PA particles has
22 been explored by using a N_2/O_2 mixture (80%/20%) as a carrier gas for the aerosol flow. The
23 particle-phase PA decay is much slower when oxygen is added in the chemical system
24 compared to the measurements without O_2 (see Fig. 5). The uptake coefficient of $\gamma_{PA}=3$ has
25 been determined and shows that the catalytic secondary reactions still govern the decay of PA
26 but the propagation length of the catalytic reactions is reduced. The decrease of the uptake
27 coefficient as a function of the oxygen concentration has been previously observed by Liu *et*
28 *al.* (Liu *et al.*, 2011) in the heterogeneous oxidation of squalane (Sq) by chlorine radicals. The
29 secondary chemistry involving Cl_2 is considered as insignificant because the ratio between O_2
30 and Cl_2 concentrations is greater than 1,000. In the presence of O_2 , a new reaction ($R^{\bullet} + O_2$)

1 competes with R2, leading to the formation of an alkyl peroxy radical instead of a chlorinated
2 radical.

3



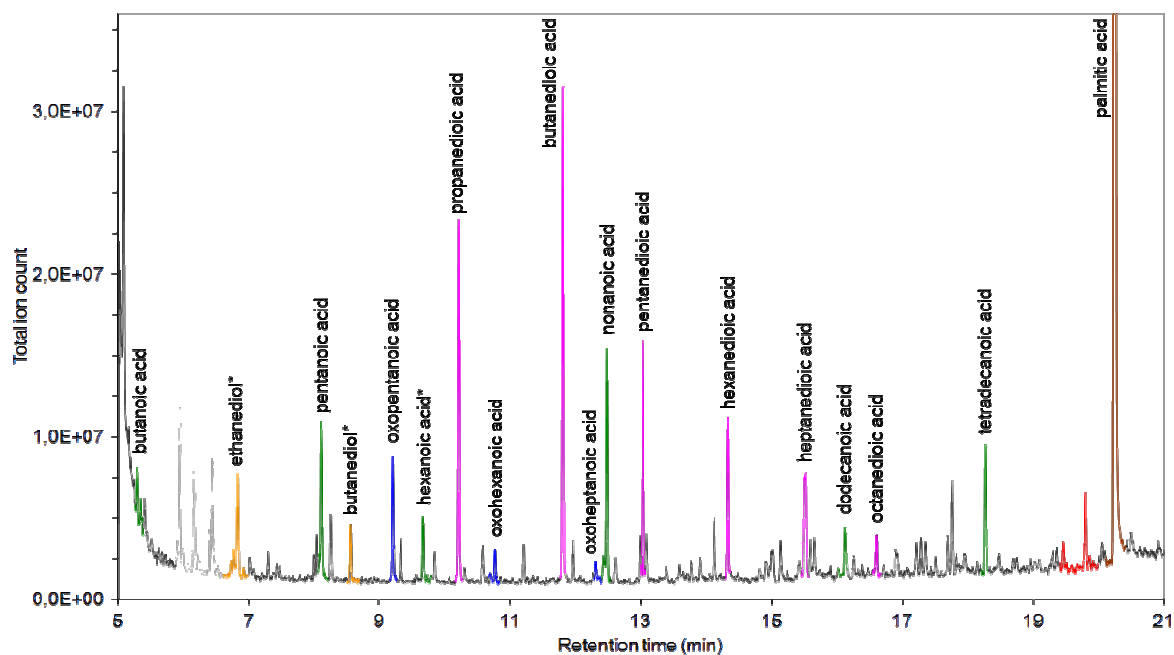
4

5 Figure 5. Normalized mass of PA remaining in the particles as a function of the chlorine
6 exposure in the presence of oxygen (squares) and the corresponding exponential fit (solid
7 line).

8 3.2.2 Particulate product identification

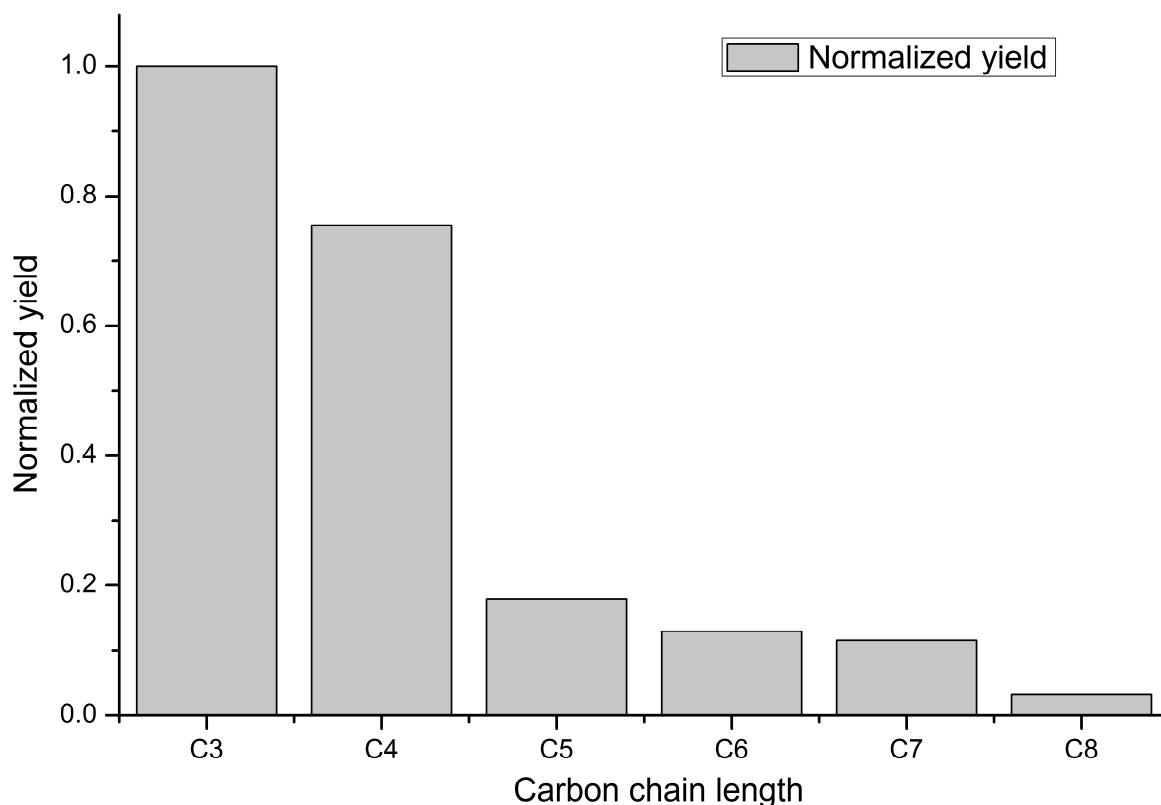
9 The products identification has been performed after the derivatization step by collecting the
10 particles at the AFT outlet during 30 minutes (see Fig. 6). We were not able to identify any
11 products on non-derivatized samples.

12 The main identified products are dicarboxylic acids and oxocarboxylic acids and confirm the
13 observations by McNeill (McNeill *et al.*, 2008) where oxocarboxylic were detected. This new
14 study allows to identify and speciate dicarboxylic and oxocarboxylic acids. Oxocarboxylic
15 acids detected are oxopentanoic, oxohexanoic and oxoheptanoic acid.



1
 2 Figure 6. Chromatogram of the silylated-products from the Cl-initiated oxidation of PA in the
 3 presence of O₂ (* uncertain identification).

4 The identification shows that the oxocarboxylic acids are produced on shorter carbon chain
 5 length than the palmitic acid but the C=O function position could not be determined in the
 6 mass spectra. Moreover, we suppose that several isomers of oxocarboxylic acids can be
 7 produced and that they may have not been separated with the gas chromatography conditions.
 8 Dicarboxylic acids have been detected from the propanedioic acid (C3) to octanedioic acid
 9 (C8). The normalized yields (Fig. 7) are calculated from the ratio of a specific dicarboxylic
 10 acid chromatographic peak area over the C3 dicarboxylic acid peak area. Those ratios are only
 11 for a comparison purpose and assume that the response coefficients are equals. The
 12 normalized yields are much higher for C3 and C4 dicarboxylic acids (Fig. 7). For that reason,
 13 oxalic acid is suspected to be produced but it has not been detected under our analytical
 14 conditions.



1
 2 Figure 7. Normalized yields of the detected dicarboxylic acids as a function of the carbon
 3 chain length.

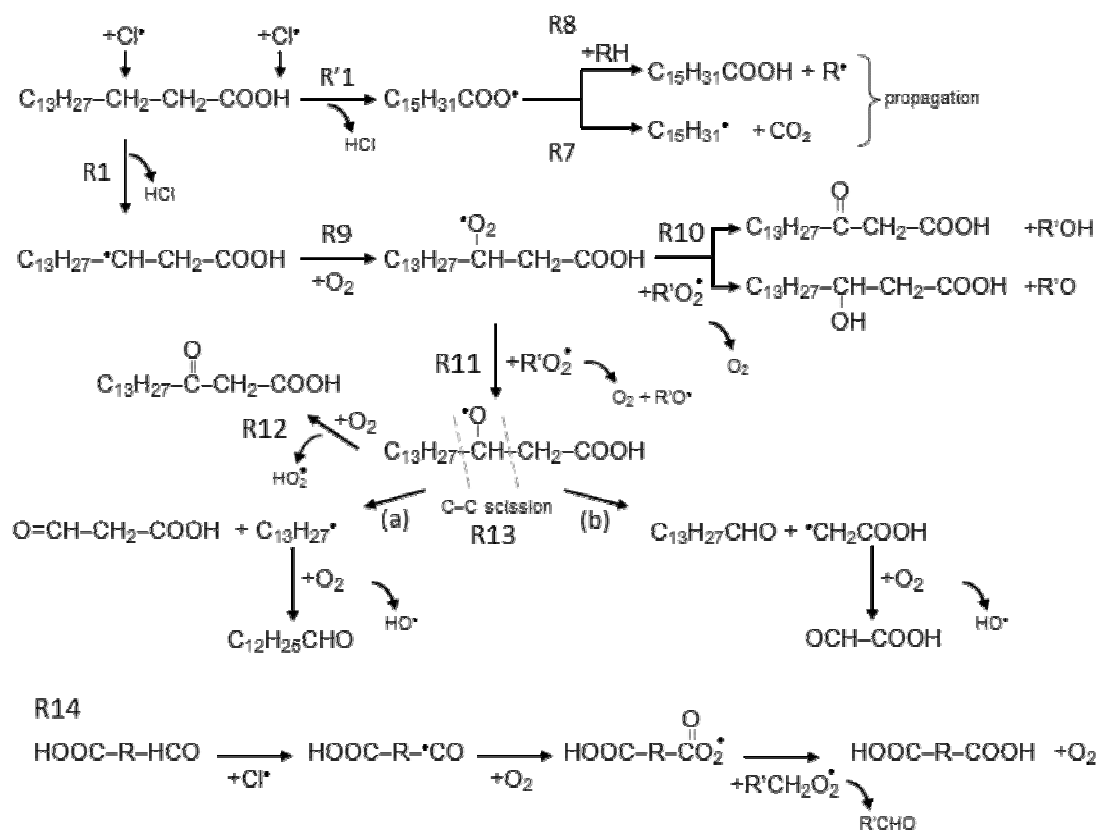
4 Products with hydroxyl functions were also detected but their formal identification cannot be
 5 guaranteed without doubt. Those products are: hydroxyethanoic acid, hydroxypropanoic acid
 6 and several diols which are consistent with the formation of hydroxyacid proposed by
 7 McNeill *et al.* (McNeill *et al.*, 2008). Monocarboxylic acids have also been detected in much
 8 lower quantities. Moreover, the gas-phase products HCl, CO₂ and CO have been clearly
 9 identified by FTIR spectroscopy by means of their characteristic fundamental bands in the
 10 case of the maximum chlorine exposure. For lower Cl^o exposure the signal to noise ratio was
 11 not sufficient even when spectra were co-added during 10 minutes.

12 3.2.3 Chemical mechanism

13 We propose a reaction mechanism (see Fig. 8) for the radical initiated oxidation of PA
 14 particles adapted from the mechanism presented by George and Abbatt (George and Abbatt,
 15 2010). We have intentionally reduced the reaction mechanism to the observed pathways based
 16 on the products identified by GC/MS. Because no relative carbon yields are suggested in our
 17 study, we cannot determine which reaction path dominates. We have chosen to show the

1 mechanism with an H-abstraction on the β position of the carboxylic function. This is for a
 2 better understanding of the mechanism and does not necessarily correspond to a preferential
 3 site of H-abstraction.

4 As in the case of the experiments without O_2 , the first step leads to the abstraction of a
 5 hydrogen atom by a Cl^\cdot radical from the aliphatic chain (R1) or from the carboxylic acid
 6 group (R'1) (Smith and Ravishankara, 2002; Singleton *et al.*, 1989). R7 is the internal
 7 recombination of $RCOO^\cdot$ to form CO_2 and the R^\cdot radical. R8 leads to the regeneration of
 8 palmitic acid. The radical $C_{15}H_{31}^\cdot$ formed on R7 will be oxidized to an alcohol, aldehyde or
 9 ultimately to a carboxylic acid.



10

11

12 Figure 8. Proposal of a reaction mechanism for the chlorine radical initiated oxidation of
 13 palmitic acid in the presence of O_2 .

14 R10 shows the recombination of RO_2^\cdot with RO_2^\cdot to form an aldehyde and an alcohol. R11
 15 leads to the formation of an alkoxy radical by recombination of two RO_2^\cdot radicals. This
 16 radical leads, via R12, to the formation of a C16 oxocarboxylic acid with the carbonyl group
 17 on the position of the initial H abstraction. The alkoxy radical recombines by C-C scission via

1 two pathways, R13(a) and (b), to form shorter chain oxocarboxylic acids and ketones
2 Formation of dicarboxylic acid is proposed on R14 to occur from an oxocarboxylic acid via H
3 abstraction on the carbonyl group and further recombination with a second peroxy radical.
4 The current study suggests that the products can also be form by any radical-initiated
5 oxidation of carboxylic acids. Moreover, the proposed mechanism is valid independently of
6 the radical (OH^\cdot or Cl^\cdot) that is involved in the H abstraction.

7 3.2.4 Discussion of previous results.

8 The values of γ determined in this work for $\text{Cl}^\cdot + \text{PA}$ are significantly higher than for
9 previously published paper for the chemical system $\text{Cl}^\cdot + \text{Squalane (Sq)}$ and $\text{Cl}^\cdot + \text{DOS}$
10 (dioctyl sebacate) heterogeneous reactions (Table 1). In the presence of oxygen, the reaction
11 is still dominated by secondary chemistry but the propagation chain length is smaller than in
12 the absence of O_2 because there is no regeneration of Cl^\cdot . In our conditions, the uptake
13 coefficient decreases by a factor of five when oxygen is added to the chemical system. This
14 result confirms the observation made by Liu *et al.* for squalane reactivity in the presence or
15 not of O_2 . Hearn and Smith study reports the opposite result where the rate of DOS loss is
16 faster in the presence of oxygen.

17 These comparisons have to be made while keeping in mind these following aspects:

18 - the chemical formula of the molecules are quite different. In the case of palmitic acid
19 (PA), the molecule exhibits a linear carbon chain with a terminal acid function contrary to
20 DOS and Squalane. As secondary chemistry is highlighted for each heterogeneous reaction,
21 the rate of propagation of these chemical reactions should be strongly dependent on the
22 chemical formula.

23 - PA is a solid while Squalane and DOS are liquid. Even if detailed chemical
24 mechanisms in the condensed phase are steel unclear, the rate of elementary processes might
25 be different for solid and liquid.

26 - the experimental determination of the uptake coefficient was not performed with the
27 same exact methodology. In previous studies the chlorine exposure, ($\langle \text{Cl}^\cdot \rangle t$), was measured
28 using reference kinetics by introducing the reference compound (2-butanone or acetone) in
29 the mixed-phase. For this, it is assumed that the atomic chlorine produced by the reaction R2
30 ($\text{R}^\cdot + \text{Cl}_2 \rightarrow \text{RCl} + \text{Cl}^\cdot_{\text{p}}$) stays in the liquid particulate phase and never returns in the gas
31 phase. So the loss of the reference compound is only due to reaction with Cl produced by the

1 photolysis of Cl₂. However, for the case of solid particle (PA), we have made the assumption
 2 that a fraction of chlorine atoms from the reaction R2 could return in the gas phase and reacts
 3 with the reference compound (acetone). For this reason, we decide to measure the chlorine
 4 exposure during an independent experiment where only acetone and Cl₂ are introduced in the
 5 AFT, so the atomic chlorine exposure determination is chlorine only generated by the
 6 photolysis of Cl₂. While chlorine exposure used in our study are in the range of the previous
 7 cited works, the contact time in the AFT is significantly different, 3 s for Cl[•] + DOS system
 8 and 180 s for our work. But recent results (Renbaum and Smith, 2011) show that radical
 9 concentration and time are interchangeable parameters only if the precursor concentrations are
 10 the same. These discrepancies with previous studies can explain at least part of our higher
 11 uptake values.

12 Table 1. Summary of measured uptake coefficients for heterogeneous reaction systems
 13 involving organic aerosol with the radical species OH[•] and Cl[•].

Uptake coefficient	OH	Cl
Squalane (C ₃₀ H ₆₂)	$\gamma_{\text{SQ}} = 0.3$ (Smith <i>et al.</i> , 2009)	$\gamma_{\text{SQ}} = 3$ in N ₂ (Liu <i>et al.</i> , 2011) $\gamma_{\text{SQ}} = 0.6$ in N ₂ /O ₂ (Liu <i>et al.</i> , 2011)
DOS ((CH ₂) ₈ (COOC ₈ H ₁₇) ₂)	$\gamma_{\text{DOS}} = 2.0$ (Hearn and Smith, 2006)	$\gamma_{\text{DOS}} = 1.7$ in N ₂ /O ₂ (Hearn <i>et al.</i> , 2007)
Palmitic acid (C ₁₆ H ₃₂ O ₂)	$\gamma_{\text{PA}} = 0.3$ (McNeill <i>et al.</i> , 2008)	$0.1 < \gamma_{\text{Cl}} < 1$ (Ciuraru, 2010) $\gamma_{\text{PA}} = 14 \pm 5$ in N ₂ $\gamma_{\text{PA}} = 3 \pm 1$ in N ₂ /O ₂

14

15

16 4 Conclusions and atmospheric implications

17 Kinetic studies have been performed to measure the uptake coefficient of chlorine atom on
 18 palmitic acid particles as a function of chlorine exposure formed by photolysis of Cl₂. The
 19 uptake coefficient has been derived from two experimental conditions (with and without O₂)

1 by measuring the palmitic acid lost from the particle phase as a function of the chlorine
2 exposure. First, we have performed these experiments in an oxygen free environment. In this
3 case, the uptake coefficient γ_{PA} is estimated to be $\gamma=14 \pm 5$. Secondly, we determined the
4 uptake coefficient in a N_2/O_2 mixture (80/20). It appears that palmitic acid loss rate as a
5 function of the chlorine exposure is lower and $\gamma_{PA} = 3 \pm 1$. It must be considered that the
6 chlorine exposure has been defined as the exposure to the chlorine atom formed only by
7 photolysis of Cl_2 and measured during separate experiments. Contrariwise, in the work of
8 Hearn *et al.* and Liu *et al.*, reference kinetics were performed simultaneously with the particle
9 oxidation considering then the chlorine atoms formed by the photolysis but also those formed
10 as products of Cl_2 dissociation due to reactivity with R^\cdot radicals. The uptake coefficient
11 determined in those studies cannot be compared directly with the uptake coefficients
12 measured in this work. Under the conditions in this study, their uptake coefficient would have
13 been greater. However, the general behaviour is similar: (1) the uptake coefficient variation is
14 a function of O_2 concentration; (2) the uptake coefficient greater than 1 explained by a
15 secondary chemistry involving radicals R^\cdot .

16 The heterogeneous reactivity experiments we performed without O_2 reveal that: (1) an
17 important secondary chemistry where Cl_2 is involved; (2) monochlorinated and
18 polychlorinated compounds are formed with up to four chlorine atoms.

19 We have observed the formation of HCl, CO and CO_2 in the gas-phase, while, in the particle-
20 phase, oxocarboxylic acids and dicarboxylic acids are detected. Alcohols and monocarboxylic
21 acids were also detected but with no certain identification of molecular formula. Dicarboxylic
22 and oxocarboxylic acids have been measured in the particulate matter by several field
23 measurement campaigns (Kawamura and Gagosian, 1987;Kawamura and Gagosian,
24 1990;Kawamura and Ikushima, 1993;Mochida *et al.*, 2002;Kawamura and Yasui, 2005;Wang
25 *et al.*, 2006;S. Kundu, 2010;Pavuluri *et al.*, 2010;Hegde and Kawamura, 2012;Mkoma and
26 Kawamura, 2013) under various environmental conditions (urban, costal, remote marine,
27 remote continental). The presence of oxocarboxylic acids is generally explained by biomass
28 combustion and the aging of primary organic matter (Kawamura and Gagosian,
29 1987;Kawamura and Gagosian, 1990;Kawamura and Yasui, 2005;S. Kundu, 2010;Pavuluri *et*
30 *al.*, 2010;Hegde and Kawamura, 2012;Mkoma and Kawamura, 2013). In this study, we
31 observed that the concentration of dicarboxylic acids seemed to decrease with the carbon
32 chain length. Similar distributions of dicarboxylic acids have been observed several times in

1 ambient particulate matter during field measurements campaigns (Kawamura and Yasui,
2 2005;S. Kundu, 2010;Pavuluri *et al.*, 2010;Hegde and Kawamura, 2012;Mkoma and
3 Kawamura, 2013). Those studies correlate the presence of dicarboxylic acids with the
4 oxidation of fatty acids and show that oxalic acid is the main dicarboxylic acid whatever the
5 origin of the analyzed samples. Those conclusions suggest that a large amount of oxalic acid
6 mass could have been formed in our experimental system although it has not been detected.

7 Finally, we have highlighted that there is a significant fragmentation and functionalization of
8 the fatty acids by oxidation initiated by radicals. This leads to the volatilization of oxygenated
9 low-molecular weight organic compounds in the atmosphere. Moreover, the functionalization
10 of the primary organic matter leads to the formation of more polar compounds at the surface
11 of the particle and suggests a modification of the hygroscopic properties of the particle. As
12 fatty acids are the most abundant identified organic compounds in the marine aerosols, the
13 aging process of those particles via radical-initiated chemistry may facilitate cloud droplet
14 activation (Westervelt *et al.*, 2012).

15 **Acknowledgements**

16 The laboratory is part of the IRENI Institute (Institut de Recherche en ENvironnement
17 Industriel) which is financed by the Nord-Pas de Calais regional council and the European
18 Regional Development Fund (FEDER). The CaPPA project (Chemical and Physical
19 Properties of the Atmosphere) is funded by the French National Research Agency (ANR)
20 through the PIA (Programme d'Investissement d'Avenir) under contract ANR-11-LABX-005-
21 01. The authors address many thanks to anonymous referees for their comments and
22 suggestions.

23 **References**

- 24 Barger, W. R., and Garrett, W. D.: Surface Active Organic Material in Air Over the
25 Mediterranean and Over the Eastern Equatorial Pacific, *J. Geophys. Res.*, 81, 3151-3157,
26 10.1029/JC081i018p03151, 1976.
- 27 Cavalli, F., Facchini, M. C., Decesari, S., Mircea, M., Emblico, L., Fuzzi, S., Ceburnis, D.,
28 Yoon, Y. J., O'Dowd, C. D., Putaud, J. P., and Dell'Acqua, A.: Advances in characterization
29 of size-resolved organic matter in marine aerosol over the North Atlantic, *J. Geophys. Res.*,
30 109, D24215, 10.1029/2004jd005137, 2004.
- 31 Ciuraru, R.: Étude de la réactivité du chlore atomique avec des particules d'aérosols d'intérêt
32 atmosphérique, 2010.

- 1 Ciuraru, R., Gosselin, S., Visez, N., and Petitprez, D.: Heterogeneous reactivity of chlorine
2 atoms with sodium chloride and synthetic sea salt particles, *Physical Chemistry Chemical*
3 *Physics*, 13, 19460-19470, 2011.
- 4 Ciuraru, R., Gosselin, S., Visez, N., and Petitprez, D.: Heterogeneous reactivity of chlorine
5 atoms with ammonium sulfate and ammonium nitrate particles, *Physical Chemistry Chemical*
6 *Physics*, 14, 4527-4537, 2012.
- 7 Docherty, K. S., and Ziemann, P. J.: On-line, inlet-based trimethylsilyl derivatization for gas
8 chromatography of mono- and dicarboxylic acids, *Journal of Chromatography A*, 921, 265-
9 275, 10.1016/s0021-9673(01)00864-0, 2001.
- 10 Donaldson, D. J., and Vaida, V.: The Influence of Organic Films at the Air–Aqueous
11 Boundary on Atmospheric Processes, *Chemical Reviews*, 106, 1445-1461,
12 10.1021/cr040367c, 2006.
- 13 Ellison, G. B., Tuck, A. F., and Vaida, V.: Atmospheric processing of organic aerosols, *J.*
14 *Geophys. Res.*, 104, 11633-11641, 10.1029/1999jd900073, 1999.
- 15 Facchini, M. C., Rinaldi, M., Decesari, S., Carbone, C., Finessi, E., Mircea, M., Fuzzi, S.,
16 Ceburnis, D., Flanagan, R., and Nilsson, E. D.: Primary submicron marine aerosol dominated
17 by insoluble organic colloids and aggregates, *GEOPHYSICAL RESEARCH LETTERS*, 35,
18 2008.
- 19 Fine, P. M., Cass, G. R., and Simoneit, B. R.: Chemical characterization of fine particle
20 emissions from fireplace combustion of woods grown in the northeastern United States,
21 *Environmental Science & Technology*, 35, 2665-2675, 2001.
- 22 Fuchs, N., and Sutugin, A.: High-dispersed aerosols, Ann Arbor Science Publishers, 1970.
- 23 Garton, D. J., Minton, T. K., Alagia, M., Balucani, N., Casavecchia, P., and Volpi, G. G.:
24 Comparative dynamics of Cl (P) and O (P) interactions with a hydrocarbon surface, *The*
25 *Journal of Chemical Physics*, 112, 5975, 2000.
- 26 George, I., Vlasenko, A., Slowik, J., Broekhuizen, K., and Abbatt, J.: Heterogeneous
27 oxidation of saturated organic aerosols by hydroxyl radicals: uptake kinetics, condensed-
28 phase products, and particle size change, *Atmospheric Chemistry and Physics*, 7, 4187-4201,
29 2007.
- 30 George, I. J., and Abbatt, J. P. D.: Heterogeneous oxidation of atmospheric aerosol particles
31 by gas-phase radicals, *Nat Chem*, 2, 713-722, 2010.
- 32 Gogou, A. I., Apostolaki, M., and Stephanou, E. G.: Determination of organic molecular
33 markers in marine aerosols and sediments: one-step flash chromatography compound class
34 fractionation and capillary gas chromatographic analysis, *Journal of Chromatography A*, 799,
35 215-231, 10.1016/s0021-9673(97)01106-0, 1998.
- 36 Hardy, J. T.: The sea surface microlayer: Biology, chemistry and anthropogenic enrichment,
37 *Progress in Oceanography*, 11, 307-328, 10.1016/0079-6611(82)90001-5, 1982.
- 38 He, L.-Y., Hu, M., Huang, X.-F., Yu, B.-D., Zhang, Y.-H., and Liu, D.-Q.: Measurement of
39 emissions of fine particulate organic matter from Chinese cooking, *Atmospheric*
40 *Environment*, 38, 6557-6564, 10.1016/j.atmosenv.2004.08.034, 2004.
- 41 He, L.-Y., Hu, M., Huang, X.-F., Zhang, Y.-H., and Tang, X.-Y.: Seasonal pollution
42 characteristics of organic compounds in atmospheric fine particles in Beijing, *The Science of*
43 *the Total Environment*, 359, 167, 2006.

1 Hearn, J. D., and Smith, G. D.: A mixed-phase relative rates technique for measuring aerosol
2 reaction kinetics, *Geophys. Res. Lett.*, 33, L17805, 10.1029/2006gl026963, 2006.

3 Hearn, J. D., Renbaum, L. H., Wang, X., and Smith, G. D.: Kinetics and products from
4 reaction of Cl radicals with dioctyl sebacate (DOS) particles in O₂: a model for radical-
5 initiated oxidation of organic aerosols, *Physical Chemistry Chemical Physics*, 9, 2007.

6 Hegde, P., and Kawamura, K.: Seasonal variations of water-soluble organic carbon,
7 dicarboxylic acids, ketoacids, and α -dicarbonyls in the central Himalayan aerosols,
8 *Atmos. Chem. Phys. Discuss.*, 12, 935-982, 10.5194/acpd-12-935-2012, 2012.

9 Kawamura, K., and Gagosian, R. B.: Implications of ω -oxocarboxylic acids in the
10 remote marine atmosphere for photo-oxidation of unsaturated fatty acids, *Nature*, 325, 330-
11 332, 1987.

12 Kawamura, K., and Gagosian, R. B.: Mid-chain ketocarboxylic acids in the remote marine
13 atmosphere: Distribution patterns and possible formation mechanisms, *Journal of*
14 *Atmospheric Chemistry*, 11, 107-122, 10.1007/bf00053670, 1990.

15 Kawamura, K., and Ikushima, K.: Seasonal changes in the distribution of dicarboxylic acids
16 in the urban atmosphere, *Environmental Science & Technology*, 27, 2227-2235,
17 10.1021/es00047a033, 1993.

18 Kawamura, K., and Yasui, O.: Diurnal changes in the distribution of dicarboxylic acids,
19 ketocarboxylic acids and dicarbonyls in the urban Tokyo atmosphere, *Atmospheric*
20 *Environment*, 39, 1945-1960, 10.1016/j.atmosenv.2004.12.014, 2005.

21 Keene, W. C., Maring, H., Maben, J. R., Kieber, D. J., Pszenny, A. A., Dahl, E. E., Izaguirre,
22 M. A., Davis, A. J., Long, M. S., and Zhou, X.: Chemical and physical characteristics of
23 nascent aerosols produced by bursting bubbles at a model air-sea interface, *JOURNAL OF*
24 *GEOPHYSICAL RESEARCH*, 112, D21202, 2007.

25 Liu, C.-L., Smith, J. D., Che, D. L., Ahmed, M., Leone, S. R., and Wilson, K. R.: The direct
26 observation of secondary radical chain chemistry in the heterogeneous reaction of chlorine
27 atoms with submicron squalane droplets, *Physical Chemistry Chemical Physics*, 13, 2011.

28 Marcolli, C., Luo, B., and Peter, T.: Mixing of the organic aerosol fractions: Liquids as the
29 thermodynamically stable phases, *The Journal of Physical Chemistry A*, 108, 2216-2224,
30 2004.

31 Marty, J. C., Saliot, A., Buat-Ménard, P., Chesselet, R., and Hunter, K. A.: Relationship
32 Between the Lipid Compositions of Marine Aerosols, the Sea Surface Microlayer, and
33 Subsurface Water, *J. Geophys. Res.*, 84, 5707-5716, 10.1029/JC084iC09p05707, 1979.

34 McNeill, V. F., Yatavelli, R. L. N., Thornton, J. A., Stipe, C. B., and Landgrebe, O.:
35 Heterogeneous OH oxidation of palmitic acid in single component and internally mixed
36 aerosol particles: vaporization and the role of particle phase, *Atmos. Chem. Phys.*, 8, 5465-
37 5476, 10.5194/acp-8-5465-2008, 2008.

38 Mkoma, S. L., and Kawamura, K.: Molecular composition of dicarboxylic acids,
39 ketocarboxylic acids, α -dicarbonyls and fatty acids in atmospheric aerosols from Tanzania,
40 East Africa during wet and dry seasons, *Atmos. Chem. Phys.*, 13, 2235-2251, 10.5194/acp-
41 13-2235-2013, 2013.

42 Mochida, M., Kitamori, Y., Kawamura, K., Nojiri, Y., and Suzuki, K.: Fatty acids in the
43 marine atmosphere: Factors governing their concentrations and evaluation of organic films on
44 sea-salt particles, *J. Geophys. Res.*, 107, 4325, 10.1029/2001jd001278, 2002.

1 Moise, T., and Rudich, Y.: Uptake of Cl and Br by organic surfaces - A perspective on
2 organic aerosols processing by tropospheric oxidants, *Geophys. Res. Lett.*, 28, 4083-4086,
3 10.1029/2001gl013583, 2001.

4 Nolte, C. G., Schauer, J. J., Cass, G. R., and Simoneit, B. R.: Highly polar organic compounds
5 present in wood smoke and in the ambient atmosphere, *Environmental Science &
6 Technology*, 35, 1912-1919, 2001.

7 O'Dowd, C. D., Facchini, M. C., Cavalli, F., Ceburnis, D., Mircea, M., Decesari, S., Fuzzi, S.,
8 Yoon, Y. J., and Putaud, J.-P.: Biogenically driven organic contribution to marine aerosol,
9 *Nature*, 431, 676-680,
10 http://www.nature.com/nature/journal/v431/n7009/supinfo/nature02959_S1.html, 2004.

11 Oliveira, C., Pio, C., Alves, C., Evtugina, M., Santos, P., Gonçalves, V., Nunes, T., Silvestre,
12 A. J. D., Palmgren, F., Wählén, P., and Harrad, S.: Seasonal distribution of polar organic
13 compounds in the urban atmosphere of two large cities from the North and South of Europe,
14 *Atmospheric Environment*, 41, 5555-5570, <http://dx.doi.org/10.1016/j.atmosenv.2007.03.001>,
15 2007.

16 Oros, D. R., and Simoneit, B. R. T.: Identification and emission factors of molecular tracers in
17 organic aerosols from biomass burning Part 2. Deciduous trees, *Applied Geochemistry*, 16,
18 1545-1565, Doi: 10.1016/s0883-2927(01)00022-1, 2001.

19 Osthoff, H. D., Roberts, J. M., Ravishankara, A. R., Williams, E. J., Lerner, B. M.,
20 Sommariva, R., Bates, T. S., Coffman, D., Quinn, P. K., Dibb, J. E., Stark, H., Burkholder, J.
21 B., Talukdar, R. K., Meagher, J., Fehsenfeld, F. C., and Brown, S. S.: High levels of nitryl
22 chloride in the polluted subtropical marine boundary layer, *Nature Geosci.*, 1, 324-328,
23 http://www.nature.com/ngeo/journal/v1/n5/supinfo/ngeo177_S1.html, 2008.

24 Pavuluri, C. M., Kawamura, K., and Swaminathan, T.: Water-soluble organic carbon,
25 dicarboxylic acids, ketoacids, and α -dicarbonyls in the tropical Indian aerosols, *J.
26 Geophys. Res.*, 115, D11302, 10.1029/2009jd012661, 2010.

27 Pechtl, S., and von Glasow, R.: Reactive chlorine in the marine boundary layer in the outflow
28 of polluted continental air: A model study, *Geophys. Res. Lett.*, 34, L11813,
29 10.1029/2007gl029761, 2007.

30 Perelygin, I. S., and Klimchuk, M. A.: Infrared spectra of coordinated acetone, *Journal of
31 Applied Spectroscopy*, 20, 687-688, 10.1007/bf00607479, 1974.

32 Renbaum, L., and Smith, G.: Artifacts in measuring aerosol uptake kinetics: the roles of time,
33 concentration and adsorption, *Atmospheric Chemistry and Physics*, 11, 6881-6893, 2011.

34 Rudich, Y.: Laboratory Perspectives on the Chemical Transformations of Organic Matter in
35 Atmospheric Particles, *Chemical Reviews*, 103, 5097-5124, 10.1021/cr020508f, 2003.

36 S. Kundu, K. K., T.W. Andreae, A. Hoffer, and M.O. Andreae: Molecular distributions of
37 dicarboxylic acids, ketocarboxylic acids and α -dicarbonyls in biomassburning aerosols:
38 implications for photochemical production and degradation in smoke layers, *Atmospheric
39 Chemistry and Physics*, 10, 2209 - 2225, 2010.

40 Schauer, J. J., Kleeman, M. J., Cass, G. R., and Simoneit, B. R. T.: Measurement of
41 Emissions from Air Pollution Sources. 3. C1-C29 Organic Compounds from Fireplace
42 Combustion of Wood, *Environmental Science & Technology*, 35, 1716-1728,
43 10.1021/es001331e, 2001.

- 1 Schauer, J. J., Kleeman, M. J., Cass, G. R., and Simoneit, B. R.: Measurement of emissions
2 from air pollution sources. 4. C1-C27 organic compounds from cooking with seed oils,
3 *Environmental Science & Technology*, 36, 567-575, 2002.
- 4 Sciare, J., Oikonomou, K., Favez, O., Liakakou, E., Markaki, Z., Cachier, H., and
5 Mihalopoulos, N.: Long-term measurements of carbonaceous aerosols in the Eastern
6 Mediterranean: evidence of long-range transport of biomass burning, *Atmos. Chem. Phys.*, 8,
7 5551-5563, 10.5194/acp-8-5551-2008, 2008.
- 8 Singleton, D. L., Paraskevopoulos, G., and Irwin, R. S.: Rates and mechanism of the reactions
9 of hydroxyl radicals with acetic, deuterated acetic, and propionic acids in the gas phase,
10 *Journal of the American Chemical Society*, 111, 5248-5251, 10.1021/ja00196a035, 1989.
- 11 Smith, I. W. M., and Ravishankara, A. R.: Role of Hydrogen-Bonded Intermediates in the
12 Bimolecular Reactions of the Hydroxyl Radical, *The Journal of Physical Chemistry A*, 106,
13 4798-4807, 10.1021/jp014234w, 2002.
- 14 Smith, J. D., Kroll, J. H., Cappa, C. D., Che, D. L., Liu, C. L., Ahmed, M., Leone, S. R.,
15 Worsnop, D. R., and Wilson, K. R.: The heterogeneous reaction of hydroxyl radicals with
16 sub-micron squalane particles: a model system for understanding the oxidative aging of
17 ambient aerosols, *Atmos. Chem. Phys. Discuss.*, 9, 3945-3981, 10.5194/acpd-9-3945-2009,
18 2009.
- 19 Spicer, C. W., Chapman, E. G., Finlayson-Pitts, B. J., Plastridge, R. A., Hubbe, J. M., Fast, J.
20 D., and Berkowitz, C. M.: Unexpectedly high concentrations of molecular chlorine in coastal
21 air, *Nature*, 394, 353-356, 1998.
- 22 Tervahattu, H., Hartonen, K., Kerminen, V.-M., Kupiainen, K., Aarnio, P., Koskentalo, T.,
23 Tuck, A. F., and Vaida, V.: New evidence of an organic layer on marine aerosols, *J. Geophys.*
24 *Res.*, 107, 4053, 10.1029/2000jd000282, 2002a.
- 25 Tervahattu, H., Juhanoja, J., and Kupiainen, K.: Identification of an organic coating on marine
26 aerosol particles by TOF-SIMS, *J. Geophys. Res.*, 107, 4319, 10.1029/2001jd001403, 2002b.
- 27 Tervahattu, H., Juhanoja, J., Vaida, V., Tuck, A. F., Niemi, J. V., Kupiainen, K., Kulmala, M.,
28 and Vehkamäki, H.: Fatty acids on continental sulfate aerosol particles, *J. Geophys. Res.*, 110,
29 D06207, 10.1029/2004jd005400, 2005.
- 30 Wang, G., Kawamura, K., Lee, S., Ho, K., and Cao, J.: Molecular, Seasonal, and Spatial
31 Distributions of Organic Aerosols from Fourteen Chinese Cities, *Environmental Science &*
32 *Technology*, 40, 4619-4625, 10.1021/es060291x, 2006.
- 33 Wang, X., Luo, L., Ouyang, G., Lin, L., Tam, N. F. Y., Lan, C., and Luan, T.: One-step
34 extraction and derivatization liquid-phase microextraction for the determination of
35 chlorophenols by gas chromatography–mass spectrometry, *Journal of Chromatography A*,
36 1216, 6267-6273, 10.1016/j.chroma.2009.07.011, 2009.
- 37 Westervelt, D., Moore, R., Nenes, A., and Adams, P.: Effect of primary organic sea spray
38 emissions on cloud condensation nuclei concentrations, *Atmos. Chem. Phys.*, 12, 89-101,
39 2012.
- 40 Yoon, Y. J., Ceburnis, D., Cavalli, F., Jourdan, O., Putaud, J. P., Facchini, M. C., Decesari, S.,
41 Fuzzi, S., Sellegri, K., Jennings, S. G., and O'Dowd, C. D.: Seasonal characteristics of the
42 physicochemical properties of North Atlantic marine atmospheric aerosols, *J. Geophys. Res.*,
43 112, D04206, 10.1029/2005jd007044, 2007.

1 Yu, J., Flagan, R. C., and Seinfeld, J. H.: Identification of Products Containing –COOH,
2 –OH, and –CO in Atmospheric Oxidation of Hydrocarbons, *Environmental Science &*
3 *Technology*, 32, 2357-2370, 10.1021/es980129x, 1998.

4 Zuo, Y., Zhang, K., and Lin, Y.: Microwave-accelerated derivatization for the simultaneous
5 gas chromatographic–mass spectrometric analysis of natural and synthetic estrogenic steroids,
6 *Journal of Chromatography A*, 1148, 211-218, 10.1016/j.chroma.2007.03.037, 2007.

7

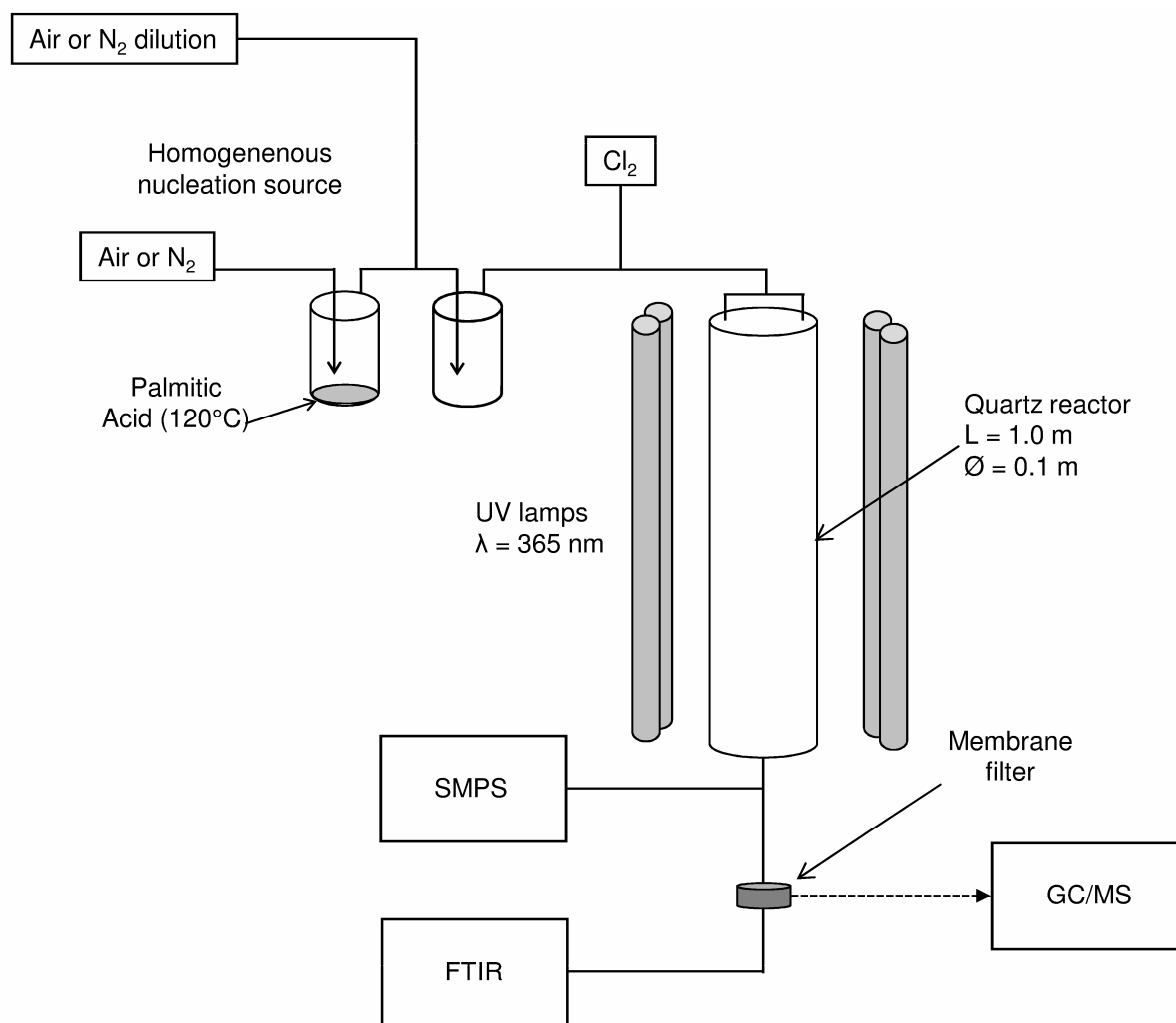
8

1 Table 1. Summary of measured uptake coefficients for heterogeneous reaction systems
 2 involving organic aerosol with the radical species OH[·] and Cl[·].

Uptake coefficient	OH	Cl
Squalane (C ₃₀ H ₆₂)	$\gamma_{\text{SQ}} = 0.3$ (Smith <i>et al.</i> , 2009)	$\gamma_{\text{SQ}} = 3$ in N ₂ (Liu <i>et al.</i> , 2011) $\gamma_{\text{SQ}} = 0.6$ in N ₂ /O ₂ (Liu <i>et al.</i> , 2011)
DOS ((CH ₂) ₈ (COOC ₈ H ₁₇) ₂)	$\gamma_{\text{DOS}} = 2.0$ (Hearn and Smith, 2006)	$\gamma_{\text{DOS}} = 1.7$ in N ₂ /O ₂ (Hearn <i>et al.</i> , 2007)
Palmitic acid (C ₁₆ H ₃₂ O ₂)	$\gamma_{\text{PA}} = 0.3$ (McNeill <i>et al.</i> , 2008)	$0.1 < \gamma_{\text{Cl}} < 1$ (Ciuraru, 2010) $\gamma_{\text{PA}} = 14 \pm 5$ in N ₂ $\gamma_{\text{PA}} = 3 \pm 1$ in N ₂ /O ₂

3

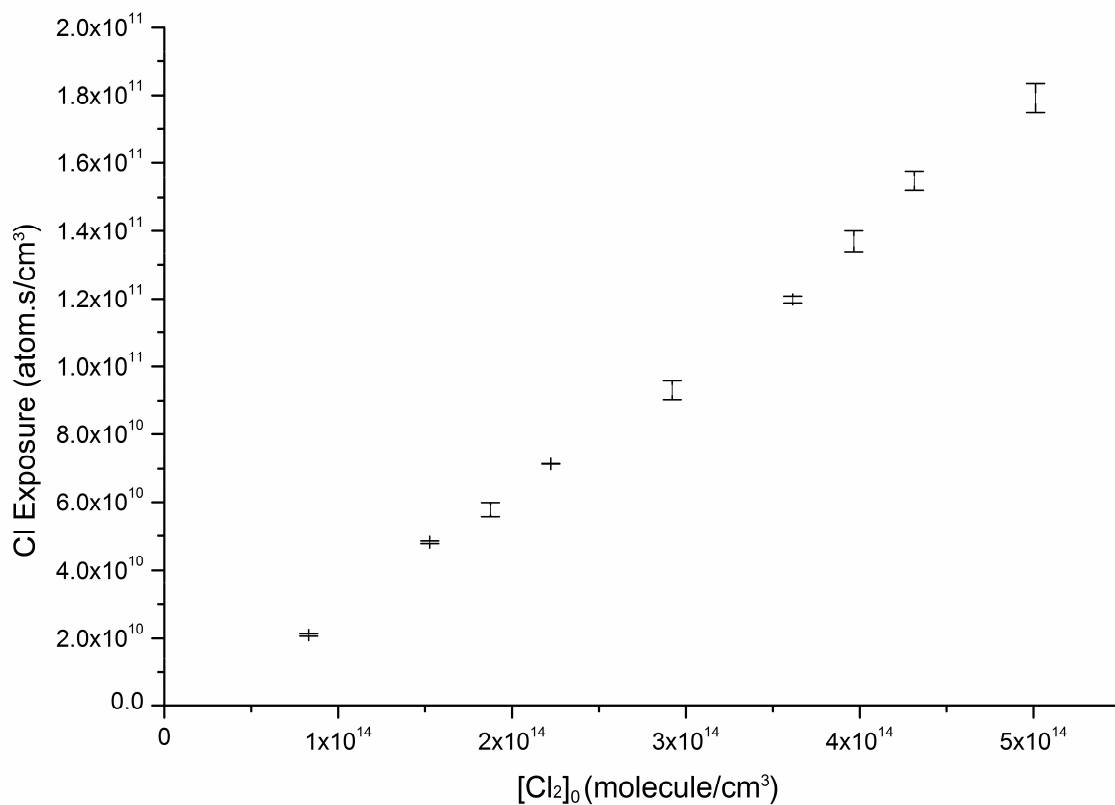
1



2

3 Figure 1. Experimental setup, SMPS (Scanning Mobility Particle Sizer), FTIR (Fourier
4 Transform InfraRed spectrometer), GC/MS (Gas Chromatography, Mass Spectrometer)

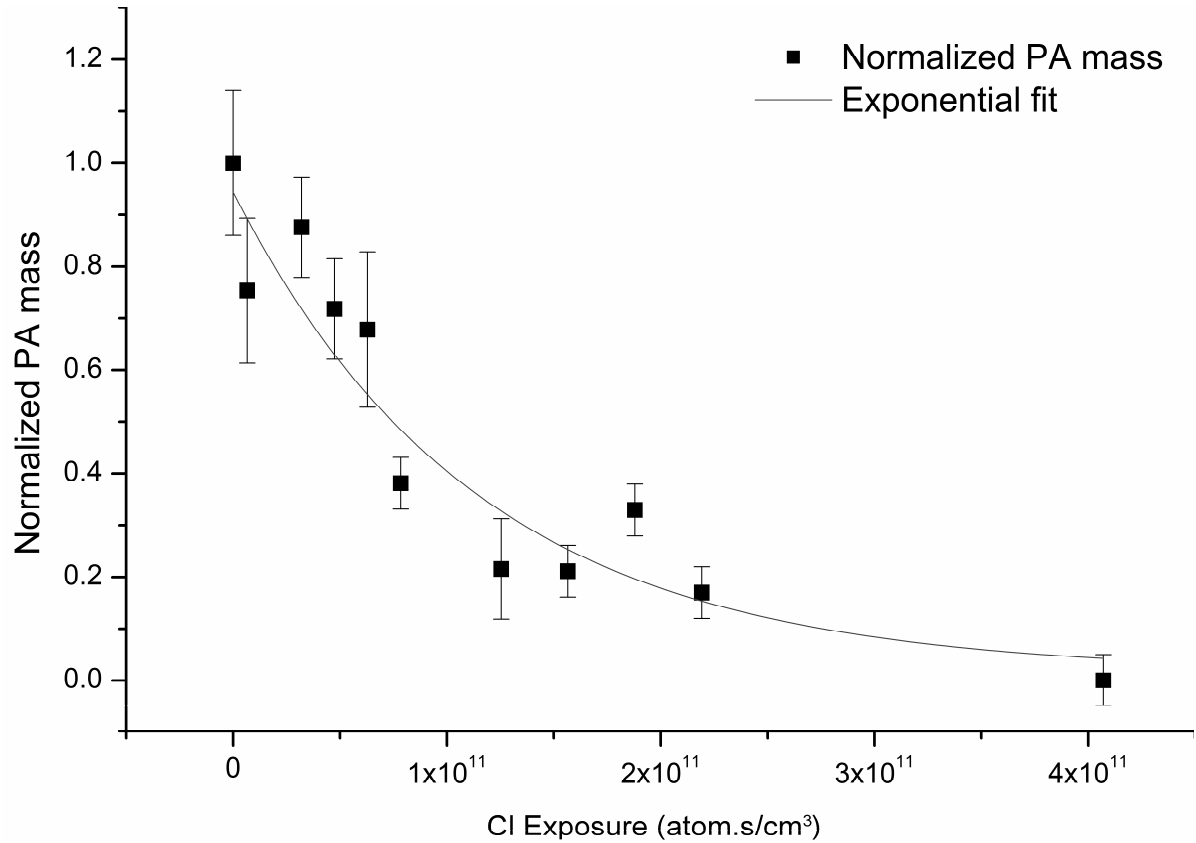
1



2

3 Figure 2. Chlorine exposure as function of the initial Cl_2 concentration in the reactor; $Q_{\text{tot}} =$
4 $4.0 \text{ L}\cdot\text{min}^{-1}$ and 8 UV lamps powered. Errors bars express the minimum and maximum values
5 of 4 experiments.

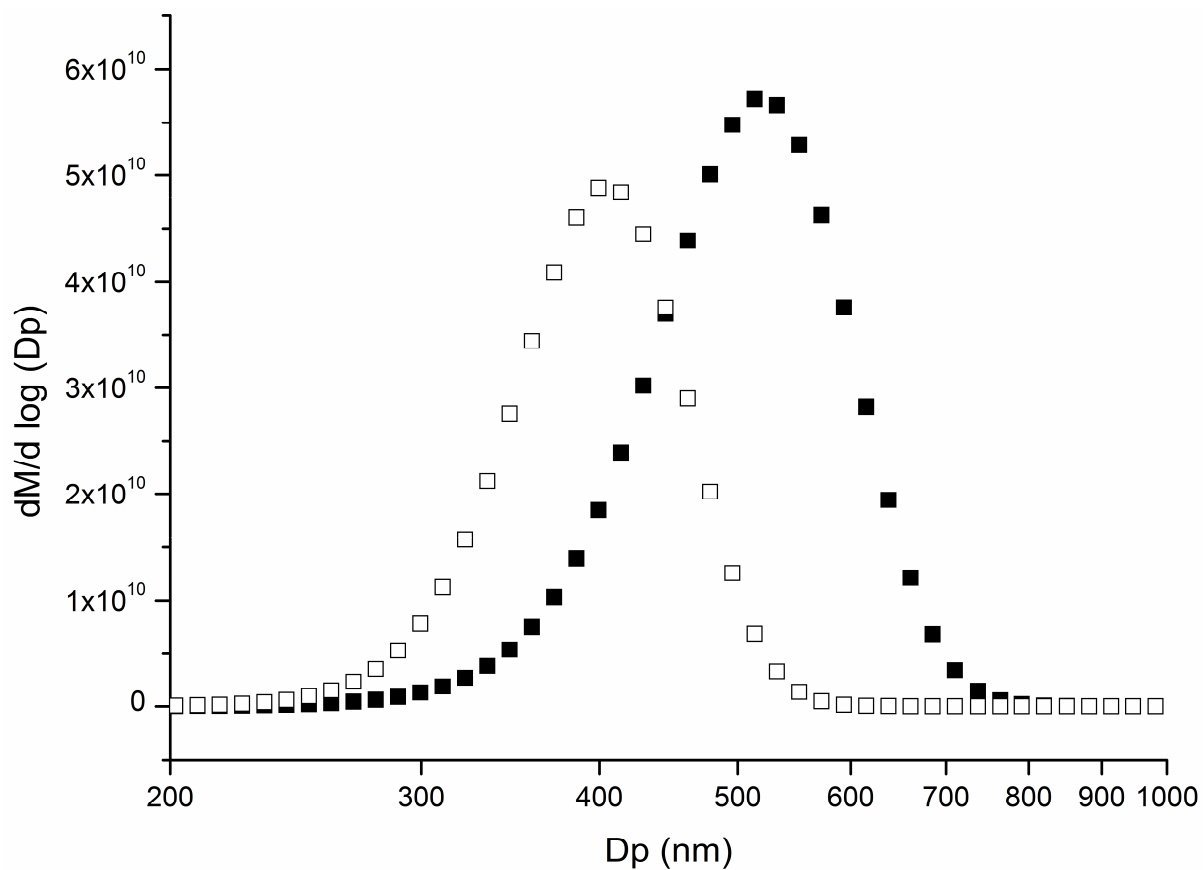
1



2

3 Figure 3. Normalized mass of PA remaining in the particles collected on filter during 10
4 minutes as a function of the chlorine exposure (squares). Each data point is the mean value
5 obtained from three GC/MS analyses of two particles samples, Errors bars represent the
6 minimum and maximum values. The data have been fitted by an exponential function (solid
7 line).

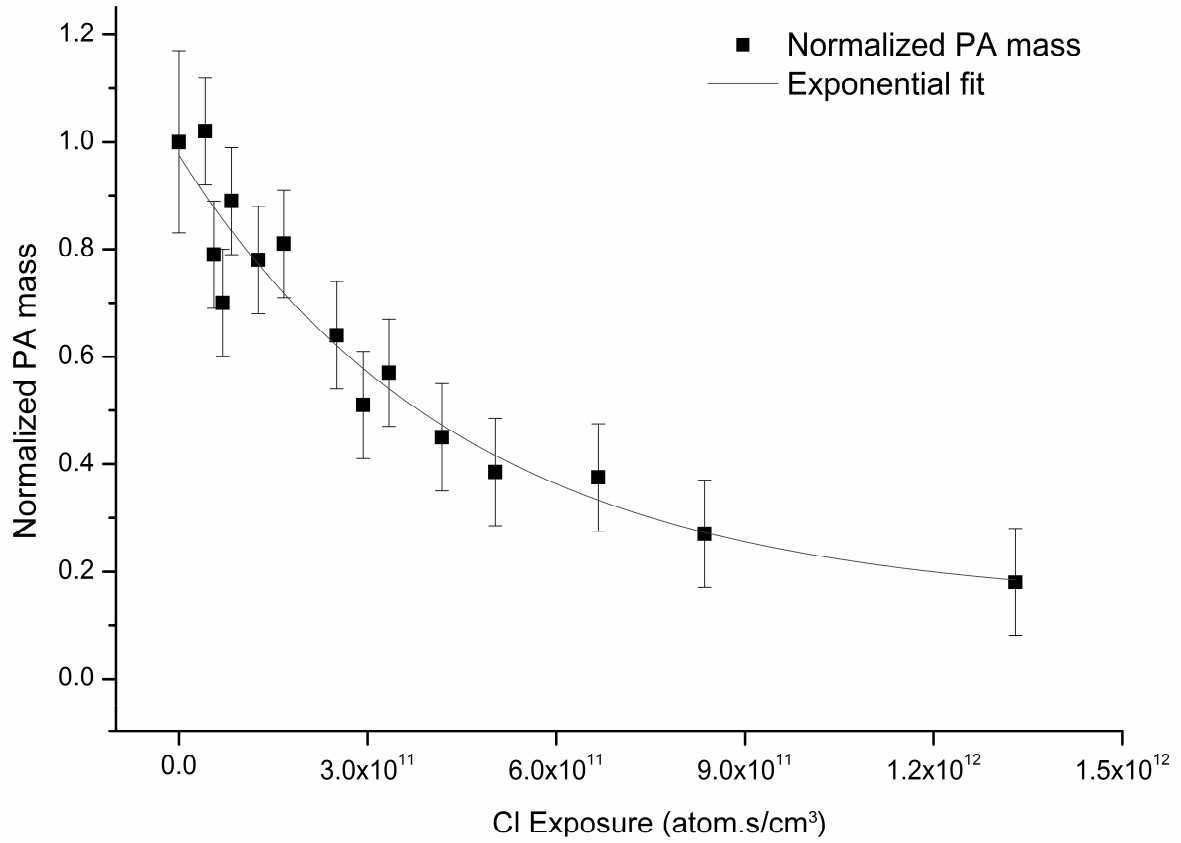
1



2

3 Figure 4. Mass-weighted particle distribution (normalized $\mu\text{g m}^{-3}$) of PA particles before
4 (filled squares) and after (open squares) a chlorine exposure of $1.25 \times 10^{11} \text{ atom.cm}^{-3}.\text{s}$. Each
5 distribution is an average of eight measurements.

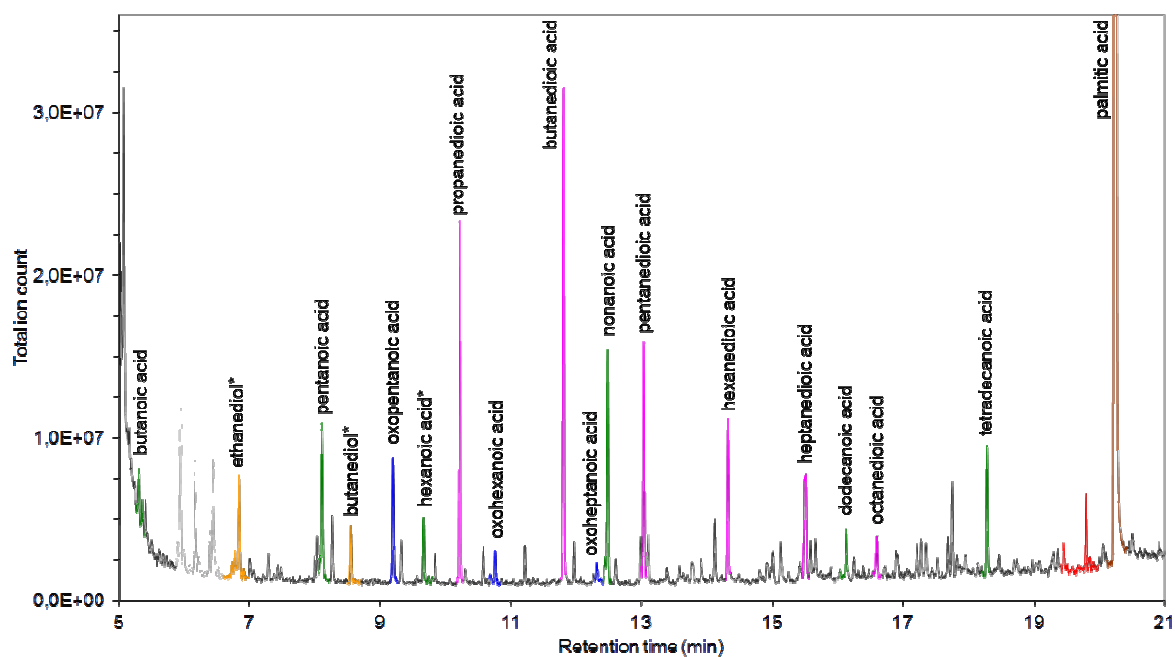
1



2

3 Figure 5. Normalized mass of PA remaining in the particles as a function of the chlorine
4 exposure in the presence of oxygen (squares) and the corresponding exponential fit (solid
5 line).

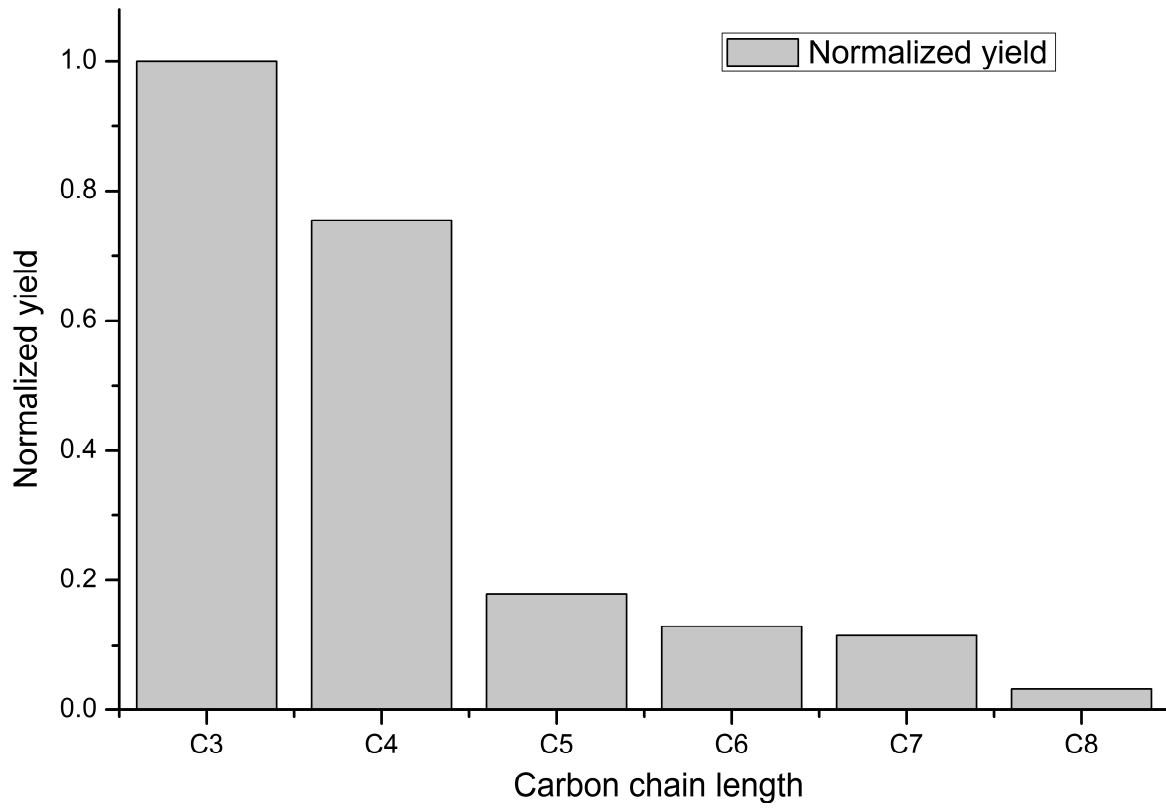
1



2

3 Figure 6. Chromatogram of the silylated-products from the Cl-initiated oxidation of PA in the
4 presence of O₂ (* uncertain identification).

1



2

3 Figure 7. Normalized yields of the detected dicarboxylic acids as function of the carbon chain
4 length.

